Czech Technical University in Prague
Faculty of Electrical Engineering
Department of Measurement

The transformation between GNSS ionospheric models

Master's Thesis

Yaroslav Kulesha

Study program: Aerospace Engineering
Branch of study: Avionics
Supervisor: doc. Dr. Ing. Pavel Kovar

Prague, May 2024

MASTER‘S THESIS ASSIGNMENT

I. Personal and study details

Student's name: **Kulesha Yaroslav** Personal ID number: **511653**

Faculty / Institute: **Faculty of Electrical Engineering**

Department / Institute: **Department of Measurement**

Study program: **Aerospace Engineering**

Branch of study: **Avionics**

II. Master’s thesis details

Master’s thesis title in English:

The transformation between GNSS ionospheric models

Master’s thesis title in Czech:

Transformace mezi GNSS ionosférickými modely

Guidelines:

Study the Klobuchar and NeQuick Ionospheric models including a simplified algorithm for calculation of the vertical ionospheric delay. Compare both models. Propose the forward and inverse algorithm (method) for transformation between model coefficients suitable for GNSS signal simulation. Verify the algorithm with the data decoded from the GPS/Galileo receiver.

Bibliography / sources:

[1] European GNSS, Galileo Open Service, Ionospheric Correction Algorithm for Galileo Single Frequency Users. http://www.gsc-europa.eu/electronic-library/programme-reference-documents
[2] European GNSS, Galileo Open Service, NTCM-G Ionospheric Model Description. http://www.gsc-europa.eu/electronic-library/programme-reference-documents
[3] GALILEO OPEN SERVICE SIGNAL-IN-SPACE INTERFACE CONTROL DOCUMENT (OS SIS ICD), Issue 2.1 | November 2023
[4] NAVSTAR GPS Space Segment/Navigation User Segment Interfaces, IS-GPS-200N

Name and workplace of master’s thesis supervisor:

doc. Dr. Ing. Pavel Kovář Department of Radioelectronics FEE

Name and workplace of second master’s thesis supervisor or consultant:

Date of master’s thesis assignment: **11.03.2024** Deadline for master's thesis submission: _____

Assignment valid until:
by the end of summer semester 2024/2025

doc. Dr. Ing. Pavel Kovář	Head of department’s signature	prof. Mgr. Petr Páta, Ph.D.
Supervisor’s signature		Dean’s signature

III. Assignment receipt

The student acknowledges that the master's thesis is an individual work. The student must produce his thesis without the assistance of others, with the exception of provided consultations. Within the master's thesis, the author must state the names of consultants and include a list of references.

. _____ _____
Date of assignment receipt Student’s signature

Thesis Supervisor:
doc. Dr. Ing. Pavel Kovar
Department of Radioelectronics
Faculty of Electrical Engineering
Czech Technical University in Prague
Technická 2
160 00 Prague 6
Czech Republic

Declaration

I declare that the presented work was developed independently and that I have listed all sources of information used within it in accordance with the methodical instructions for observing the ethical principles in the preparation of university theses.

In Prague, May 2024

.....
Yaroslav Kulesha

Abstract

Largest source of errors in global navigation satellite system (GNSS) positioning is ionosphere. To mitigate signal delays as they travel through Earth's ionosphere, ionospheric correction models were developed. European Union's Galileo system employs a complex and more accurate NeQuick model, while United State's Global Positioning System (GPS) relies on a simple straightforward Klobuchar model. This thesis investigates the possibilities of transformation between two different ionospheric models.

The research focuses on developing a method for converting model coefficients enabling flexibility between the models. Real-world data obtained from GPS/Galileo receivers was used in modeling the ionospheric delays for both models. A set of uniformly distributed around the globe user positions was employed to access the difference between the models. The difference between real and transformed coefficients for the models was investigated.

This study contributes to understanding the relationship between two fundamentally different models used in different navigation systems. The transformation has the potential to facilitate the development of more accurate ionospheric error correction techniques and improve performance of GNSS-based applications.

Keywords: GNSS, ionospheric error, ionospheric delay, Klobuchar model, NeQuick model, space weather effects on satellite navigation, GPS/Galileo receiver data decoding, coefficients transformation.

Acknowledgements

I sincerely thank my supervisor, Dr. Pavel Kovar, for the opportunity to work under his guidance and for the valuable support he provided during my studies. I extend my gratitude to the Government of the Czech Republic for the continuous scholarship funding I received throughout my studies at the Czech Technical University in Prague. I am grateful to the Czech Technical University in Prague and the Erasmus+ Programme for providing me with the opportunity to participate in a student exchange program in my field of study at Yildiz Technical University in Istanbul, Turkey. I sincerely thank the Czech Technical University in Prague and Yildiz Technical University for the knowledge I gained during my time at both institutions. Last, but certainly not least, I express my deepest gratitude to my family and friends for their unwavering love and support throughout my journey.

List of Tables

List of Figures

List of Acronyms

ASICTP Abdus Salam International Centre for Theoretical Physics. 10

CCIR International Radio Consultative Committee. 15

ECEF Earth-centered, Earth-fixed. 20, 24, 28, 32, 35

GEO geostationary orbit. 21

GNSS global navigation satellite system. 1–4, 7–10, 14, 16–19, 27, 28, 30, 46

GPS Global Positioning System. 1, 3, 5, 9, 18, 20, 22, 28, 29, 44

ICTP International Centre for Theoretical Physics. 10

ITU-R Radiocommunication Sector of the International Telecommunication Union. 15

LEO low Earth orbit. 21

MEO medium Earth orbit. 21–23

MODIP Modified Dip Latitude. 11, 12

RINEX Receiver Independent Exchange Format. 19, 29, 30, 36

RMS root mean square. 1

RTK real-time kinematic. 10

STEC Slant Total Electron Content. 12–14, 30

TECU Total Electron Content Units. 14, 31

UT Universal Time. 2, 29

Contents

Chapter 1

Introduction

The ionosphere, a region of the Earth's atmosphere is characterized by free electron density and plays an important role in global navigation satellite system (GNSS) signal propagation. When GNSS signal travels through ionosphere, it is delayed due to interaction with the free electrons. Results of such interactions effecting the accuracy and bring errors in positioning of receivers.[1] Influence of ionosphere is the largest source of errors in satellite positioning. To access the ionospheric delays, different models have been developed. Every model is designed with different complexity and uses different and distinct mathematical formulations and sets of parameter that represent the behavior of the ionosphere.[2], [3]

Two such models are the Klobuchar and NeQuick ionospheric models. The Klobuchar model is based on empirical approach[4] reduces about 50% root mean square (RMS) ionospheric range error worldwide. It uses a first-order approximation of the ionospheric delay by modeling the ionosphere as a simple single-layer shell at a fixed height of 350 km. The slant delay is computed from vertical delay at the pierce point of the ionosphere multiplied by an obliquity factor. Global Positioning System (GPS) utilizes this model by broadcasting 8 parameters from the satellites. The model is suitable for real-time applications with limited computational resources, in particular for single-frequency GNSS receivers. However, model's accuracy is limited during periods of high solar activity, in regions with complex ionospheric structures, or at low angles of elevation where.[5]

The NeQuick model provides a more complex and sophisticated approach of the ionosphere's electron density profile using a set of three coefficients broadcasted from Galileo satellites. The model employs a function based on ionospheric layers to describe the density of electrons in different altitudes. It offers an improved accuracy compared to simpler Klobuchar model.[5] NeQuick model is adopted by the Galileo system for its single-frequency users. The model predicts monthly mean electron density, which depends

on input values that depend on solar activity: solar flux, month, geographic coordinates, altitude and Universal Time (UT). The model has capabilities to provide vertical and slant ionospheric error correction by integration of the predicted electron density along the line of sight between receiver and satellite.[3]

The coexistence of these diverse models with their own strengths and limitations, presents opportunities and challenges. Each model serves a specific purpose and brings different accuracy. [6] Their lack of direct interchangeability obstruct the seamless integration of data across diverse GNSS applications, such as multi-constellation GNSS processing[7], ionospheric studies[5], or GNSS signal simulations[8]. Different GNSS constellations utilize different ionospheric models. Transfoming between these models is important to eachieve an optimal performance in multi-constellation GNSS receivers. Often, researches need to compare or combine data derived from different models, which is requiring a reliable method for converting between models parameters. Lastly, GNSS signal simlators often rely on one single ionospheric model, which is limiting their ability to realistically represent the wide range of potential ionospheric conditions seen in the real-world scenarios.

This research is devoted to find a method for possible transformation between the Klobuchar and NeQuick ionospheric models. The accuracy of the method is evaluated under a range of ionospheric conditions. This work may contribute to a more reliable GNSS-based applications. The outcomes of this research hold a potential for advancement of our understanding of the ionosphere modeling, as well as increasing the accuracy of GNSS technologies in different scientific and engineering domains.

Chapter 2

Theoretical part

2.1 Klobuchar model

2.1.1 Introduction to the Klobuchar model

The Klobuchar model, developed by John Klobuchar in the fourth quarter of previous century was designed as a relatively simple, but effective way for estimating ionospheric delays.[4] This model was developed for the GPS system gained wide acceptance and is implemented in many GNSS receivers due to its simplicity and minimal computational requirements. It makes the model suitable for resource-constrained devices.

The model uses 8 coefficients that are broadcasted from the GPS satellites within the navigation message. The model utilizes a simplified representation of the ionosphere various behavior. The coefficients capture the global characteristics of the ionosphere at a given time. Then, model uses these coefficients with the user's geographic location and observation time to compute the estimated ionospheric delay.

Despite its simplicity, Klobuchar model has advantages which make it easily adaptable for practical usage. The model uses parameters that are found in daily navigation messages from satellites. Klobuchar model provides acceptable accuracy and allows in precise positioning especially in mid-latitudes.

It is important to say, that Klobuchar model as any other has its restrictions. One of the restrictions is that the model does not take into account all complex phenomena that are found in ionosphere and relies on relatively simple slant factor calculation. Vertical and slant delay illustration of the Klobuchar model can be seen on figure 2.1.

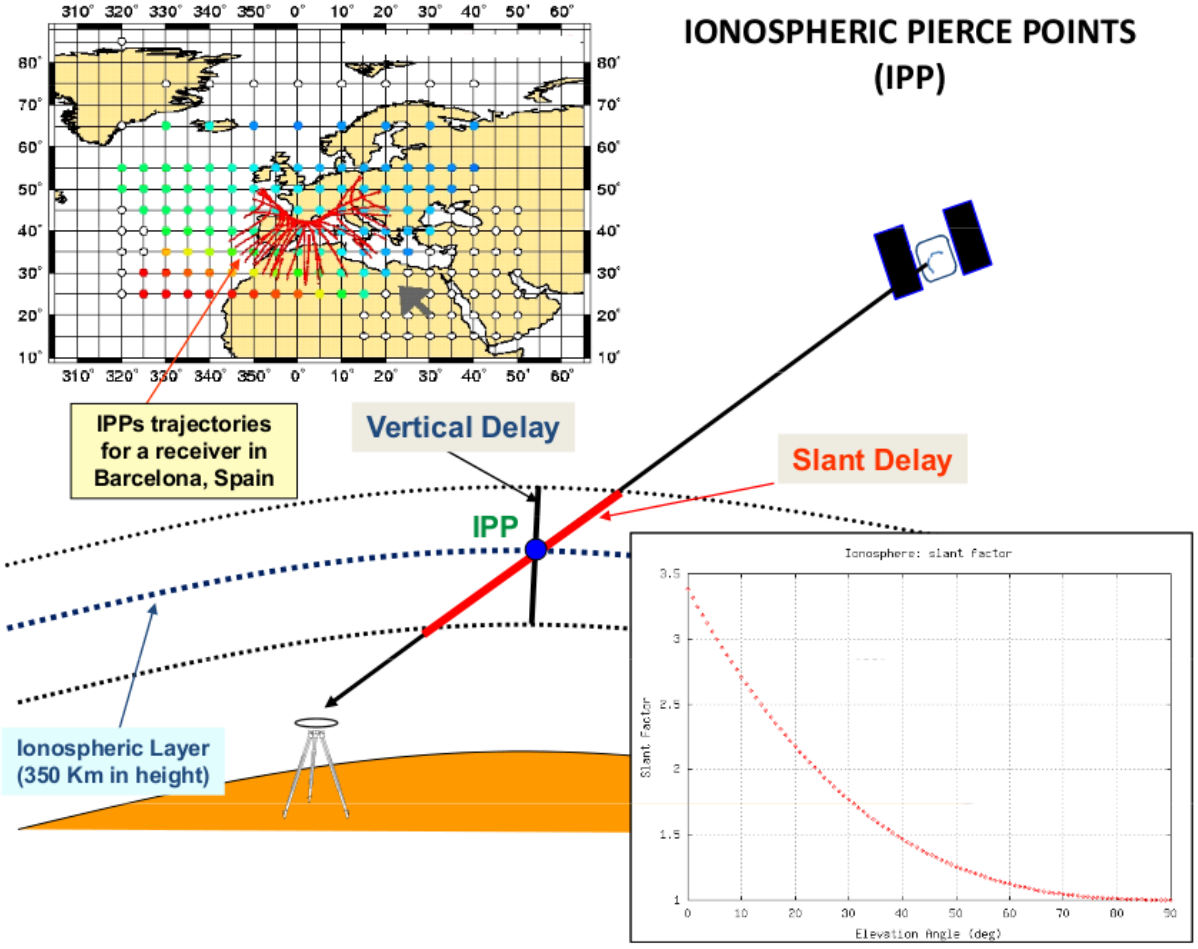

Figure 2.1: Vertical and slant delay illustration of the Klobuchar model

The figure at bottom right shows the obliquity factor variation with the elevation of ray.

In this section, a close look at the Klobuchar model is taken. The subsequent sections will provide a deeper understanding in the mathematical formulation of the Klobuchar model, analyze its parameters, and discuss its strengths and limitations in greater detail.

2.1.2 Mathematical formulation of the Klobuchar model

The model expresses the vertical ionospheric delay, *Tiono*, as a function of geomagnetic latitude, local time at the ionospheric pierce point, and eight model parameters. These parameters are broadcast within the navigation message of GNSS satellites and are updated typically every few hours to reflect the dynamic nature of the ionosphere.

The calculation of the ionospheric delay involves several steps and takes inputs such as user latitude and longitude, viewing a GPS satellite at Azimuth and Elevation angles, as well as time and transmitted coefficients[2]:

1. Calculating Earth-centered angle:

$$\psi = \frac{0.0137}{E + 0.11} - 0.022, \text{ [semicircles]} \tag{2.1}$$

2. Determining the subionospheric latitude:

$$\Phi_I = \Phi_u + \psi \cos(A) \tag{2.2}$$

3. Determining the subionospheric longitude:

$$\lambda_I = \lambda_u + \frac{\psi \sin(A)}{\cos(\Phi_i)} \tag{2.3}$$

4. Finding the geomagnetic latitude:

$$\Phi_m = \Phi_I + 0.064 \cos(\lambda_I - 1.617) \tag{2.4}$$

5. Calculating Local Time at the ionospheric pierce point:

$$t = 4.32 \times 10^4 \lambda_I + \text{GPS time}, \text{ [s]} \tag{2.5}$$

6. Determining the slant factor:

$$F = 1 + 16(0.53 - E)^3 \tag{2.6}$$

7. Computing the ionospheric time delay:

$$T_{\text{iono}} = F \left(5 \times 10^{-9} + \alpha \left(1 - \frac{X^2}{2} + \frac{X^4}{24} \right) \right), \text{ [ns]} \tag{2.7}$$

where

$$\alpha = \alpha(1) + \alpha(2) \cdot \Phi_m + \alpha(3) \cdot \Phi_m^2 + \alpha(4) \cdot \Phi_m^3 \tag{2.8}$$

and

$$X = \frac{2\pi(t - 50400)}{\beta} \tag{2.9}$$

and

$$\beta = \beta(1) + \beta(2) \cdot \Phi_m + \beta(3) \cdot \Phi_m^2 + \beta(4) \cdot \Phi_m^3 \tag{2.10}$$

Algorithm layout of the Klobuchar model can be seen on figure 2.2.

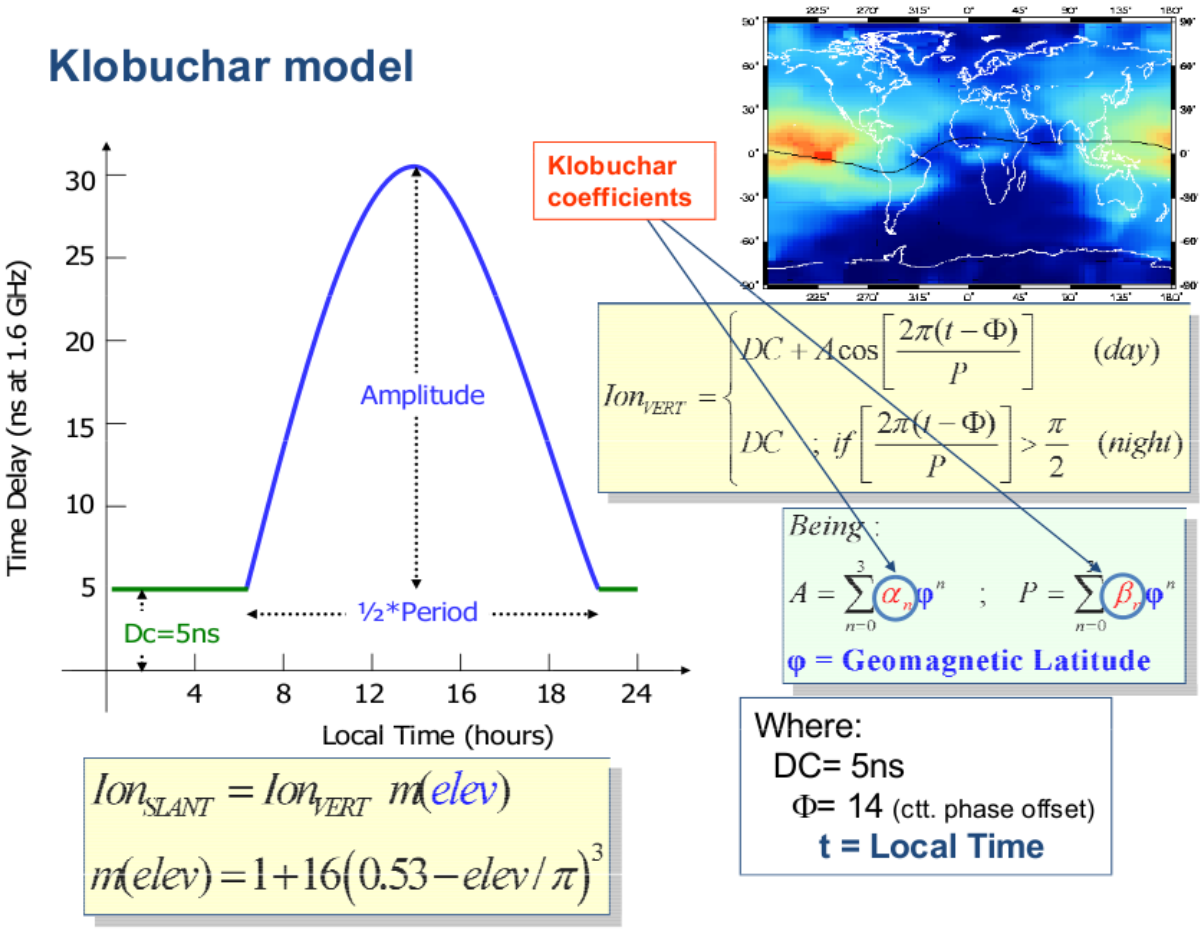

Figure 2.2: Klobuchar model

2.1.3 Klobuchar model parameters

The Klobuchar model, despite its simplicity, relies on eight parameters to estimate ionospheric delay. These parameters, broadcast within the navigation message of GNSS satellites, are crucial for accurate positioning and time synchronization.

The eight parameters are typically denoted as α_1, α_2, α_3, α_4, β_1, β_2, β_3, and β_4. These parameters are not static but rather change with time and are updated periodically in the navigation message. The α parameters represent the amplitude of the ionospheric delay variation, while the β parameters determine the period of this variation.

The parameters α_1 and α_2 primarily govern the amplitude of the diurnal variation in ionospheric delay. This diurnal variation, strongly influenced by the sun's position, results in higher electron density and consequently larger ionospheric delays during daytime hours. α_1 controls the overall magnitude of the diurnal variation. Higher values of α_1 indicate a more pronounced difference between daytime and nighttime ionospheric delays. α_2 introduces a latitudinal dependence on the amplitude. Its value modulates the effect of α_1 based on the user's latitude, reflecting the fact that the ionosphere's behavior varies with geographic location.

While α_1 and α_2 address daily changes, α_3 and α_4 capture the seasonal variations in ionospheric behavior. The ionosphere tends to be denser and more variable during periods of high solar activity, typically coinciding with specific seasons. α_3 reflects the overall impact of seasonal changes on ionospheric delay. A larger α_3 suggests a more significant difference in delay between seasons with high and low solar activity. α_4, similar to α_2, introduces a latitude-dependent scaling to the seasonal effect. This accounts for variations in seasonal behavior of the ionosphere at different latitudes.

The parameters β_1 and β_2 define the period of the diurnal variation in ionospheric delay. Instead of directly representing time, these parameters influence the rate at which the delay changes throughout the day. β_1 dictates the base period of the diurnal variation. A larger β_1 corresponds to a slower rate of change in delay, meaning the transition between minimum and maximum delay occurs over a longer period. β_2 introduces a latitude-dependent adjustment to the period, similar to the role of α_2 for amplitude. This recognizes that the duration of maximum ionospheric delay can vary depending on the user's latitude.

Analogous to the diurnal parameters, β_3 and β_4 control the period of the seasonal

variation in ionospheric delay. These parameters influence how quickly the ionosphere transitions between periods of high and low activity throughout the year. β_3 sets the fundamental period of the seasonal variation. A larger β_3 corresponds to a slower transition between periods of high and low ionospheric delay, signifying a more gradual change in seasonal effects. β_4, similar to β_2, allows for a latitude-dependent fine-tuning of the seasonal period, acknowledging that the duration of high ionospheric activity can differ across latitudes.

2.1.4 Advantages and limitations of the Klobuchar model

Main advantage of the Klobuchar model is its simplicity, however simplicity also brings certain limitations when compared to more sophisticated models like NeQuick.

With only eight parameters and a straightforward algorithm, it enables quick and efficient calculation of ionospheric delays, even on devices with limited processing power. This aspect was particularly crucial in the early days of GNSS when receiver technology was not as advanced.

The model's simplicity translates directly into ease of implementation. The straightforward mathematical formulation and minimal parameter requirements make it easy to integrate into various GNSS software and hardware platforms. This facilitated its widespread adoption, ensuring that even basic receivers could account for ionospheric effects.

The Klobuchar model, through its eight global parameters transmitted in the navigation message, provides a first-order approximation of ionospheric delay for any location on Earth. This global coverage makes it suitable for applications requiring basic ionospheric corrections without dependence on regional or local models.

The eight Klobuchar parameters are readily available in the broadcast navigation message transmitted by GNSS satellites. This eliminates the need for users to acquire external ionospheric data, simplifying receiver design and operation.

The simplicity of the Klobuchar model, while advantageous for computation, compromises its accuracy, especially during periods of high ionospheric activity. It often oversimplifies the complex physical processes within the ionosphere, leading to larger residual errors compared to more sophisticated models.

The model relies on a static snapshot of the ionosphere, represented by the eight global parameters updated infrequently. This fails to capture the dynamic nature of the ionosphere, neglecting temporal and spatial variations that can significantly impact delay estimations.

The Klobuchar model's accuracy deteriorates significantly during periods of heightened solar and geomagnetic activity. These events induce rapid fluctuations in the ionosphere, which the model, with its static representation, cannot adequately capture.

The model exhibits reduced accuracy at low elevation angles where the signal path through the ionosphere is longer. This limitation stems from the model's simplified assumptions about the ionosphere's structure, which are less valid at lower elevations.

The reliance on broadcast parameters, while convenient, can be a drawback. The parameters, updated only a few times a day, may not reflect the current ionospheric conditions accurately, leading to reduced correction accuracy.

The global nature of the Klobuchar model prevents it from capturing localized, small-scale variations in the ionosphere. These variations, although less impactful than large-scale effects, can still contribute to significant errors in precise positioning applications.

Compared to the NeQuick model, the Klobuchar model trades accuracy for computational efficiency. While Klobuchar relies on a simplified approach with global parameters, NeQuick utilizes a more complex, physically-based model with parameters derived from a global ionospheric grid. This allows NeQuick to provide higher accuracy, especially during challenging ionospheric conditions. However, this comes at the cost of increased computational burden, making NeQuick less suitable for resource-constrained platforms.[7]

2.1.5 Applications of Klobuchar model

The primary application of the Klobuchar model is in single-frequency GNSS receivers, which constitute a significant portion of receivers used in mass-market applications like navigation systems and location-based services. These receivers primarily operate on a single frequency band (e.g., L1 for GPS) and are most susceptible to ionospheric delays. The Klobuchar model provides a readily available correction factor transmitted within the navigation message, enabling these receivers to mitigate ionospheric errors and achieve improved positioning accuracy.

While real-time kinematic (RTK) techniques typically employ more sophisticated ionospheric modeling approaches, the Klobuchar model can still play a role in certain scenarios. For instance, in the initialization phase of RTK, where ambiguity resolution is yet to be achieved, the Klobuchar model can provide an initial estimate of ionospheric delay, aiding in faster convergence to a solution. Additionally, in challenging environments where communication interruptions occur, the Klobuchar model can act as a fallback option to provide continuous, albeit less accurate, positioning information.

Although not its primary purpose, the Klobuchar model can be used for basic ionospheric studies and monitoring. By analyzing the variation of Klobuchar model parameters over time and location, researchers can gain insights into the behavior and variability of the ionosphere. This information is valuable for understanding space weather phenomena and their potential impact on GNSS signals and other radio communication systems.

Due to its relative simplicity and ease of implementation, the Klobuchar model serves as a valuable tool for educational purposes. It provides students and researchers new to GNSS and ionospheric studies with a tangible example of an ionospheric model and its application in mitigating positioning errors. Additionally, the model's straightforward formulation makes it an ideal starting point for developing and testing new algorithms or techniques related to ionospheric modeling and correction.

The Klobuchar model finds application in GNSS signal simulation and testing environments. By incorporating the model into simulation software, developers can generate realistic GNSS signals that account for the effects of the ionosphere. This capability is crucial for evaluating the performance of new receiver designs, algorithms, and positioning techniques under various simulated ionospheric conditions.

2.2 NeQuick model

2.2.1 Introduction to the NeQuick model

The NeQuick model stands as a widely recognized empirical model designed to characterize the electron density distribution within the Earth's ionosphere. Its development arose from a collaborative endeavor between the International Centre for Theoretical Physics (ICTP) and the Abdus Salam International Centre for Theoretical Physics (ASICTP), aiming to provide a computationally efficient yet accurate representation of ionospheric

behavior. Unlike some models that focus on specific regions or conditions, NeQuick offers global coverage, making it suitable for a wide range of applications, from precise satellite navigation to understanding ionospheric variability.[3]

The NeQuick model's foundation rests on a representation of the ionosphere as a series of layers, each characterized by a specific electron density profile. This layered approach allows for a more realistic depiction of the ionosphere's complex structure compared to simpler models. Moreover, NeQuick incorporates readily available geophysical parameters, such as solar radio flux and geomagnetic indices, to account for the dynamic nature of the ionosphere, influenced by factors like solar activity and geomagnetic storms.

Its computational efficiency, coupled with its relative accuracy, has positioned NeQuick as a valuable tool within the broader field of ionospheric modeling and applications that rely on understanding the ionosphere's impact on radio wave propagation. This subchapter delves deeper into the mathematical framework, input parameters, and applications of the NeQuick model, providing a comprehensive understanding of its capabilities and limitations.

2.2.2 Mathematical formulation of the NeQuick model

The NeQuick model utilizes a layered approach to represent the electron density profile of the ionosphere. It divides the ionosphere into layers, each characterized by a specific mathematical function describing the electron density variation with altitude.

To determine the electron density N at a specific location identified by the coordinates h, ϕ, λ and time, utilizing the Effective Ionisation Level Az derived from coefficients a_0, a_1, a_2 broadcasted daily from satellites, and the receiver's Modified Dip Latitude (MODIP), all NeQuick parameters must be evaluated. MODIP regions can be seen on figure 2.3

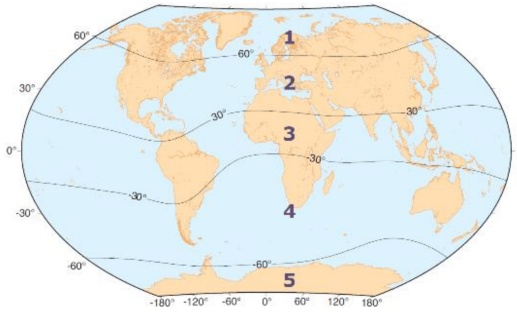

Region 1	60 deg < *MODIP* ≤ 90 deg
Region 2	30 deg < *MODIP* ≤ 60 deg
Region 3	−30 deg ≤ *MODIP* ≤ 30 deg
Region 4	−60 deg ≤ *MODIP* < −30 deg
Region 5	−90 deg ≤ *MODIP* < −60 deg

Figure 2.3: MODIP regions associated to different ionospheric characteristics

The Effective Ionisation Level, Az, is determined as follows:

$$\mathrm{Az} = \alpha_0 + \alpha_1 \times \mathrm{MODIP} + \alpha_2 \times (\mathrm{MODIP})^2 \tag{2.11}$$

MODIP is expressed in degrees in a table for every geographical location and is provided together with the NeQuick model. The receiver then calculates the integrated Slant Total Electron Content (STEC) along the path using NeQuick model and converts it to slant delay using next equation:

$$d_{\mathrm{igr}} = \frac{40.3}{f^2} \cdot \mathrm{STEC} \tag{2.12}$$

where d_{igr} is the group delay (m), f is frequency (Hz), N is electron density (electrons/m^3), STEC (electrons/m^2).

Even though ionosphere is divided to four layers, D, E, F1, F2, NeQuick utilizes two layers that influence the ionosphere error the most. Bottomside layer represents the lower part of the ionosphere, typically extending up to the F2 layer peak, which exists from about 220 to 800 km above the surface of the Earth.

Topside layer extends from the F2 layer peak upwards where the electron density gradually decreases. In the topside ionosphere, NeQuick adopts a simplified approach. It assumes a constant electron density gradient above a specific altitude, typically around 1000 km. Structure of the ionosphere can be seen on figure 2.4.

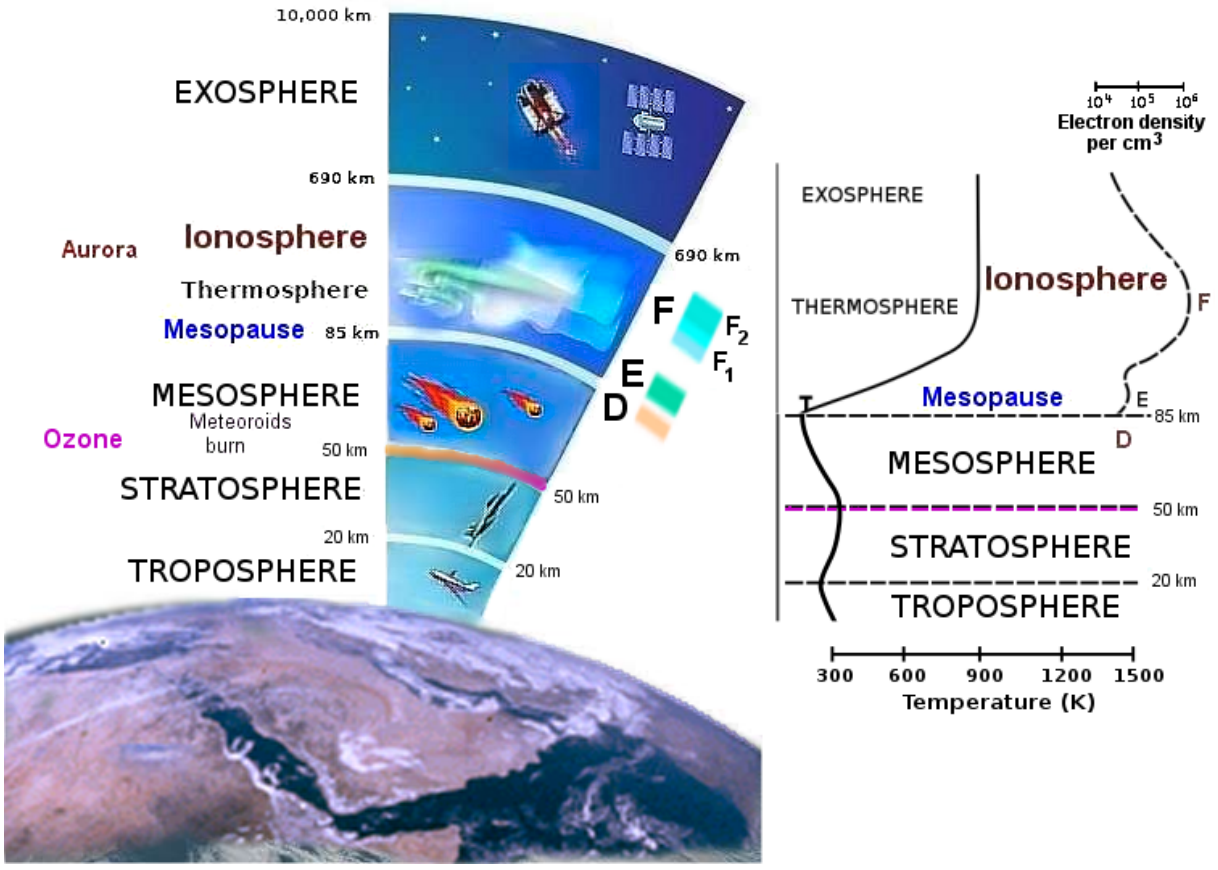

Figure 2.4: Atmosphere structure

To ensure a continuous electron density profile across layer boundaries, NeQuick employs specific constraints that ensure a smooth transition between the bottomside and topside representations.

To compute the STEC along a stragith line between receiver and satellite antennas, the NeQuick electron density must be evaluated at some point along the signal path. The coordinates of the point depend on the receiver's computation capabilities to identify the number of points where N is evaluated. It is for required to obtain sufficient accuracy for the further computation, leading to the STEC. Geometry representation of the point discussed above can be seen on 2.5.

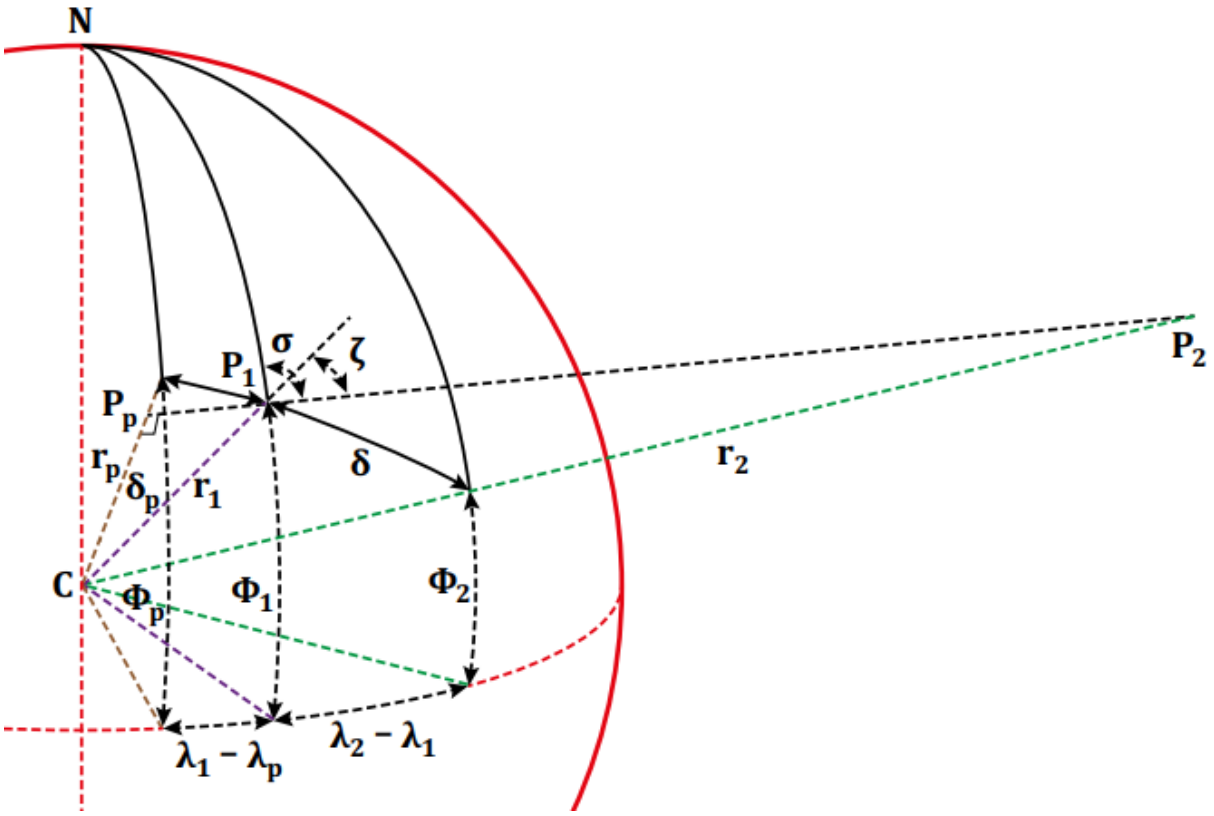

Figure 2.5: Geometry of the NeQuick computation

STEC is expressed in units of Total Electron Content Unites (TECU), where 1 Total Electron Content Units (TECU) eqauls 10^{16} electrons/m^2.

By employing this layered structure and mathematical framework, NeQuick can provide a reasonably accurate representation of the electron density distribution within the ionosphere.[5] Detailed implementation of the NeQuick model can be found at the European GNSS Service Centre.[3]

Example of a global vertical TECU map generated with NeQuick model can be seen on figure 2.6

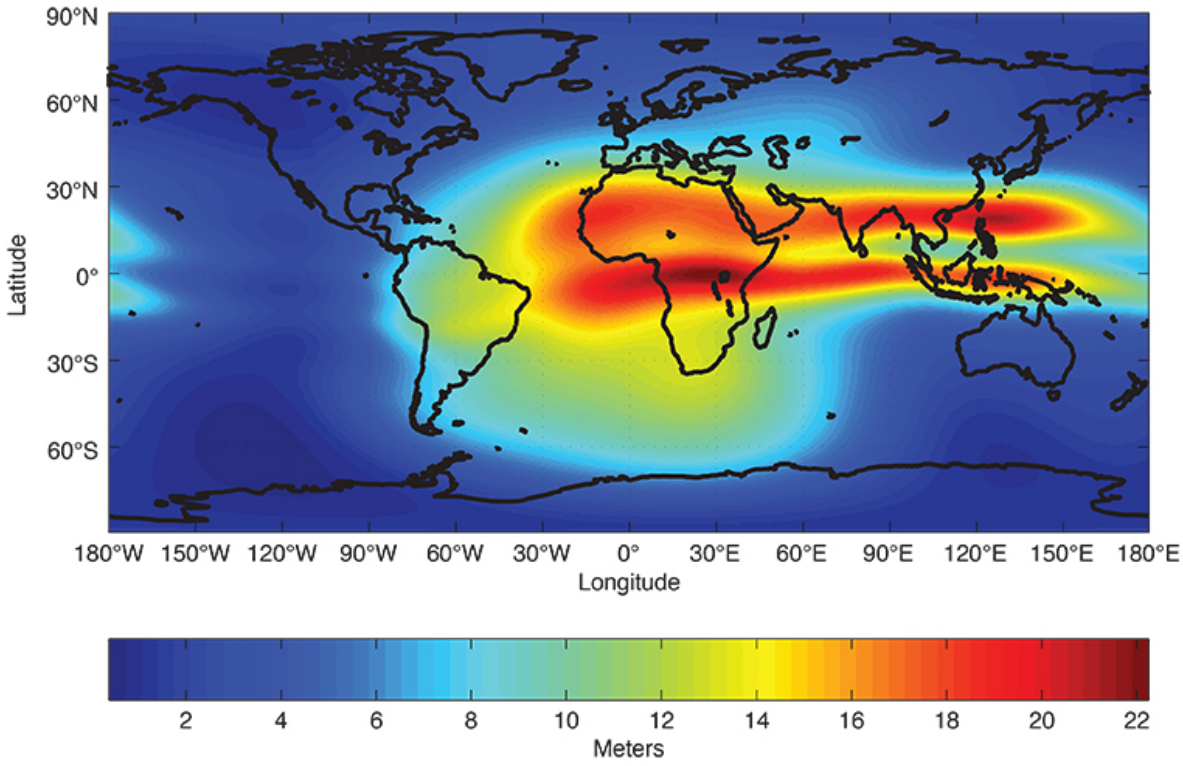

Figure 2.6: Global vertical Total Electron Content map generated with NeQuick model

2.2.3 NeQuick model parameters

NeQuick model utilizes a set of coefficients, (α_0, α_1, α_2), to represent the zenith total electron content at a reference point. These coefficients play a crucial role in shaping the overall TEC profile predicted by the model.

The three coefficients are typically obtained from two primary sources: navigation messages and International Radio Consultative Committee (CCIR) data files supplied with the model.

Galileo constellation broadcast these coefficients within their navigation messages. This direct dissemination ensures users have access to up-to-date ionospheric information for improved positioning accuracy.

The CCIR, now known as the Radiocommunication Sector of the International Telecommunication Union (ITU-R), provides files containing predicted values for the coefficients. These files, generated using historical data and ionospheric models, offer a broader temporal and spatial coverage.

These coefficients provide crucial information about the ionosphere's state at a given time and location. They capture the temporal dynamics of the ionosphere, which are essential for accurate GNSS positioning and other applications sensitive to ionospheric delays.

However, it is important to note that the coefficients represent a simplified representation of the ionosphere's complex behavior. Their accuracy relies on the quality of the underlying data used for their derivation and might not fully capture rapid ionospheric fluctuations, especially during periods of heightened solar activity.[9]

2.2.4 Advantages and limitations of the NeQuick model

NeQuick exhibits good accuracy in representing the ionosphere's variability under different solar and geomagnetic conditions, demonstrating consistent performance across diverse geographical regions.

For example, in the figure 2.7 performance of Klobuchar and NeQuick models is shown. NeQuick model overperforms more simple Klobuchar model. Improvement is most noticeable in periods of weak ionospheric activity, when NeQuick 29% better than Klobuchar model.[5] This is particularly valuable for GNSS applications, which require accurate ionospheric delay estimations across a wide range of user positions. Furthermore, the NeQuick model demonstrates good accuracy in representing ionospheric electron density under various solar and geophysical conditions. Its dependence on the effective solar radio flux index allows it to adapt to varying levels of solar activity, a crucial factor influencing ionospheric behavior. [5]

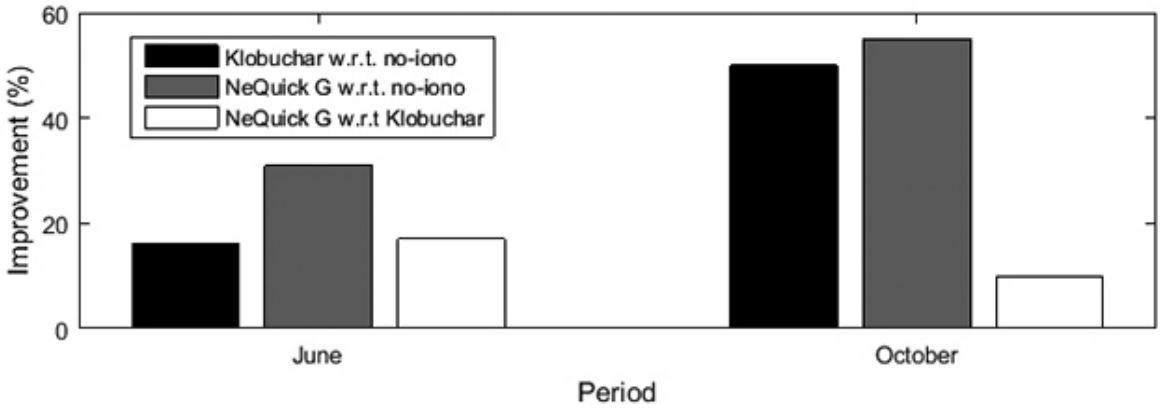

Figure 2.7: Position estimate improvement over Brazil region

Despite these strengths, NeQuick model is relatively complex compared to the Klobuchar model. It requires higher computational power from the receivers.Furthermore, the model's accuracy can be affected by regional variations in ionospheric behavior, which are not fully accounted for in its global parameterization. For instance, studies have shown that the NeQuick model might exhibit biases in equatorial regions, particularly during periods of high ionospheric scintillation. [3]

2.2.5 Applications of NeQuick model

NeQuick model primarily is used in Galileo constellation for correction due to ionosphere. Beyond GNSS, NeQuick finds utility in ionospheric studies and space weather forecasting. Its ability to model electron density profiles globally makes it valuable for understanding ionospheric variability and its drivers, including solar activity and geomagnetic storms. Researchers use NeQuick to study phenomena like ionospheric scintillation, which can disrupt radio communication and navigation signals.[7]

NeQuick proves valuable in radio wave propagation analysis and prediction. Its ability to model electron density profiles over a range of altitudes and geographic locations allows for accurate prediction of radio wave propagation paths and signal strength. This proves essential for various applications, including high-frequency (HF) communication, over-the-horizon radar, and remote sensing techniques that rely on signals traversing the ionosphere. [10]

Chapter 3

Practical part

3.1 GNSS constellations

Since Klobuchar and NeQuick models are designed for specific constellations, in this work, two of the GNSS constellations were observed: GPS (fig. 3.1)) and Galileo (3.2)). This approach is important because both Klobuchar and NeQuick models rely on constellation-specific parameters for ionospheric delay estimation. Analyzing data from these constellations allows for a comparative assessment of the models performance across different signal characteristics. This will can provide insights into the strengths and limitations of each model in different operational environments.

Figure 3.1: Global Positioning System

Figure 3.2: Galileo GNSS

Ephemeris data is crucial for precise positioning in GNSS. It provides information about the precise location of satellites in their orbits, which allows receivers to calculate their own position accurately.

There are two main types of ephemeris data. First is transmitted directly from satellites as a part of their navigation message. It provides a good accuracy, ususally in meters range, but is less precise than precise ephemeris. Precise ephemeris is determined by ground stations tracking the satellites orbits. Accuracy of such ephemeris is up to centimeters range.

Receiver Independent Exchange Format (RINEX) is a standard file format for exchanging the GNSS observation data. Ephemeris data is one type of information stored within RINEX files. In the work scope, Keplerian parameters were used to find the positions of constellations such as semi-majox axis, eccentricity, inclination, right ascension of the ascending node, argument of perigee, mean anomaly. RINEX files also contain parameteres for ionospheric correction. Example of the RINEX structure which was used for further computing is shown on 3.3

```
     3.04           N: GNSS NAV DATA    M: MIXED            RINEX VERSION / TYPE
MergeMNfile.tcl     IGS                 20240418 153505 GMT PGM / RUN BY / DATE
BDSA   2.7940E-08  5.9605E-07 -3.9935E-06  6.1989E-06 U 02  IONOSPHERIC CORR
BDSA   2.7940E-08  6.4075E-07 -4.4107E-06  7.2122E-06 W 05  IONOSPHERIC CORR
BDSA   2.7940E-08  6.4075E-07 -4.4107E-06  7.2122E-06 W 06  IONOSPHERIC CORR
...
BDSA  -9.3132E-09 -6.8545E-07  1.1921E-07  3.3379E-06 D 50  IONOSPHERIC CORR
BDSB   1.2083E+05  3.6045E+05 -4.2598E+06  5.8327E+06 U 02  IONOSPHERIC CORR
BDSB   1.6589E+05 -5.8982E+05  2.1627E+06 -3.2768E+05 W 05  IONOSPHERIC CORR
...
BDSB  -1.8842E+05 -7.5366E+05 -7.3400E+06  4.1288E+06 D 50  IONOSPHERIC CORR
GAGP  1.8335413188E-09 1.332267630E-14 259200 2310          TIME SYSTEM CORR
GAL    1.3825E+02 -4.6875E-02  1.5808E-02                   IONOSPHERIC CORR
GPSA   3.6322E-08  7.4506E-09 -1.7881E-07 -5.9605E-08       IONOSPHERIC CORR
GPSB   1.3926E+05  3.2768E+04 -3.2768E+05  3.2768E+05       IONOSPHERIC CORR
QZSA   1.0245E-08 -1.4901E-08 -4.1723E-07  1.1921E-06       IONOSPHERIC CORR
QZSB   1.0240E+05  0.0000E+00 -8.5197E+05  8.3231E+06       IONOSPHERIC CORR
BDSA   2.7940E-08  6.4075E-07 -4.4107E-06  7.2122E-06 W 60  IONOSPHERIC CORR
BDSB   1.6589E+05 -5.8982E+05  2.1627E+06 -3.2768E+05 W 60  IONOSPHERIC CORR
GAUT  1.8626451492E-09-8.881784197E-16 172800 2310          TIME SYSTEM CORR
GPUT -3.7252902985E-09-7.993605777E-15 503808 2310          TIME SYSTEM CORR
GLUT  3.2596290112E-09 0.000000000E+00      0    0          TIME SYSTEM CORR
QZUT -1.8626451492E-09 0.000000000E+00 356352 2158          TIME SYSTEM CORR
BDUT -3.7252902985E-09 0.000000000E+00 259145  954          TIME SYSTEM CORR
    18    18  1929     7                                    LEAP SECONDS
                                                            END OF HEADER
G02 2024 04 17 00 00 00-4.521366208790E-04 6.480149750130E-12 0.000000000000E+00
     6.800000000000E+01 3.568750000000E+01 4.447328106210E-09 2.174921610440E-01
     1.782551407810E-06 1.603420171890E-02 7.113441824910E-06 5.153705919270E+03
     2.592000000000E+05-1.322478055950E-07 2.689277950010E+00-1.788139343260E-07
     9.676164993050E-01 2.503437500000E+02-1.202931742410E+00-8.321775206770E-09
     5.428797559780E-11 1.000000000000E+00 2.310000000000E+03 0.000000000000E+00
     2.000000000000E+00 0.000000000000E+00-1.769512891770E-08 6.800000000000E+01
     2.520180000000E+05 4.000000000000E+00
G02 2024 04 17 02 00 00-4.520895890892E-04 6.480149750132E-12 0.000000000000E+00
     7.000000000000E+01 3.650000000000E+01 4.379468136712E-09 1.267693422942E+00
     1.640990376472E-06 1.603394642007E-02 7.176771759987E-06 5.153704723358E+03
     2.664000000000E+05 1.452863216400E-07 2.689218219065E+00-4.023313522339E-07
     9.676182840655E-01 2.440000000000E+02-1.202972159911E+00-8.029977337931E-09
     1.139333172086E-10 1.000000000000E+00 2.310000000000E+03 0.000000000000E+00
     2.000000000000E+00 0.000000000000E+00-1.769512891769E-08 7.000000000000E+01
     2.592180000000E+05 4.000000000000E+00
```

Figure 3.3: Example of a file containing ionospheric correction parameters

Ephemeris data from GPS and Galileo constellations at 02:00 UTC on 17.04.2024 was decoded. Coordinates in geodetic and Earth-centered, Earth-fixed (ECEF) coordinate systems were found for each satellite of each constellation.

Figure 3.4 represents ECEF coordinates (x, y, z) shown in relation to latitude and longitude.

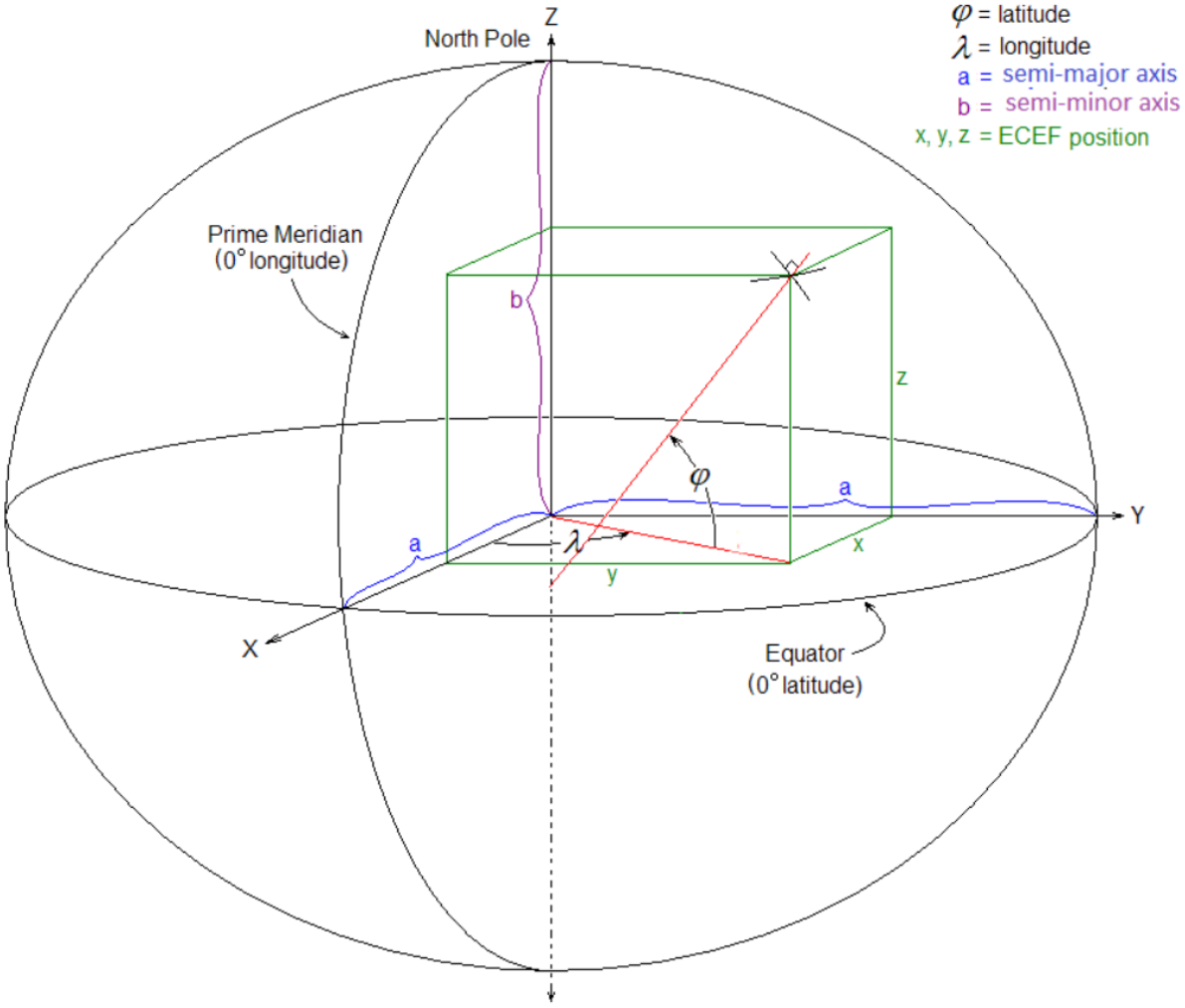

Figure 3.4: The ECEF coordinates (x, y, z) shown in relation to latitude and longitude

3.1.1 Medium Earth orbit

A medium Earth orbit (MEO) is a type of orbit that is located between low Earth orbit (LEO) and geostationary orbit (GEO). MEO satellites circle the Earth at altitudes between 2000 and 35786 kilometers, making them higher than LEO satellites but lower than GEO satellites. This positioning grants them a unique set of advantages, primarily a wider coverage area than LEO satellites and lower latency than GEO satellites.

MEO orbits are particularly well-suited for navigation systems like GPS, as they allow for a greater number of satellites to be tracked simultaneously, enhancing accuracy and reliability. MEO satellites are also used for telecommunications, providing broadband internet access to remote regions and contributing to global connectivity.

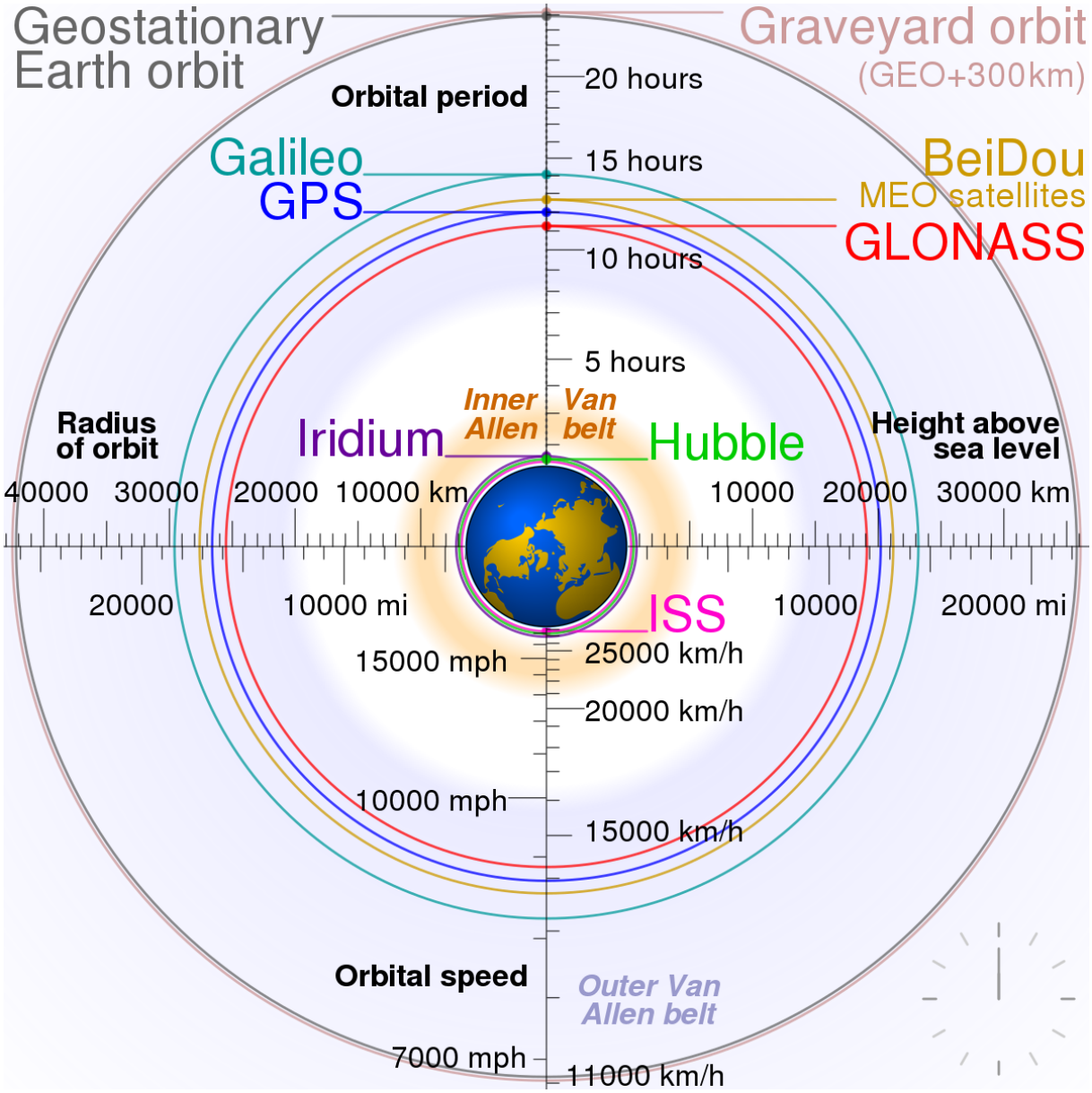

Figure 3.5: Comparison of satellite navigation orbits

3.1.2 GPS constellation

GPS constellation currently consists of 31 operational satellites in MEO. Satellites positions for further calculations are showed in the figure 3.6.

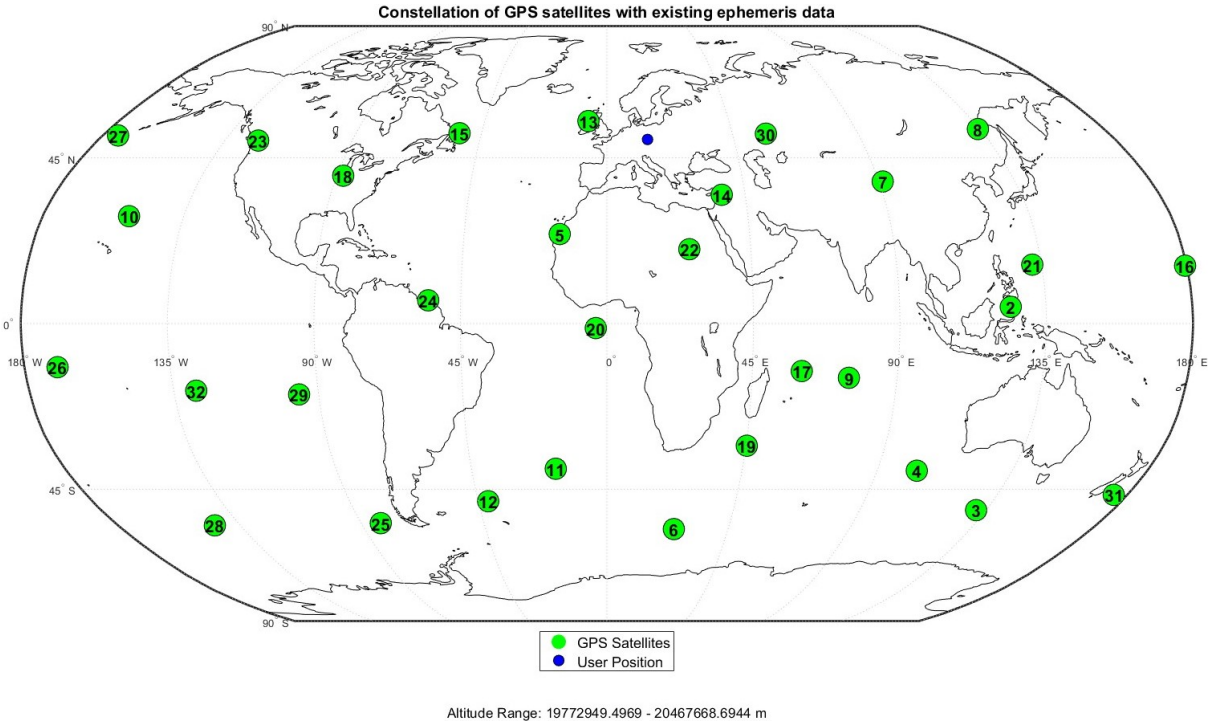

Figure 3.6: GPS constellation

3.1.3 Galileo constellation

Galileo aims for 30 operational satellites in MEO. Active 23 satellites for further calculation are showed in the figure 3.7.

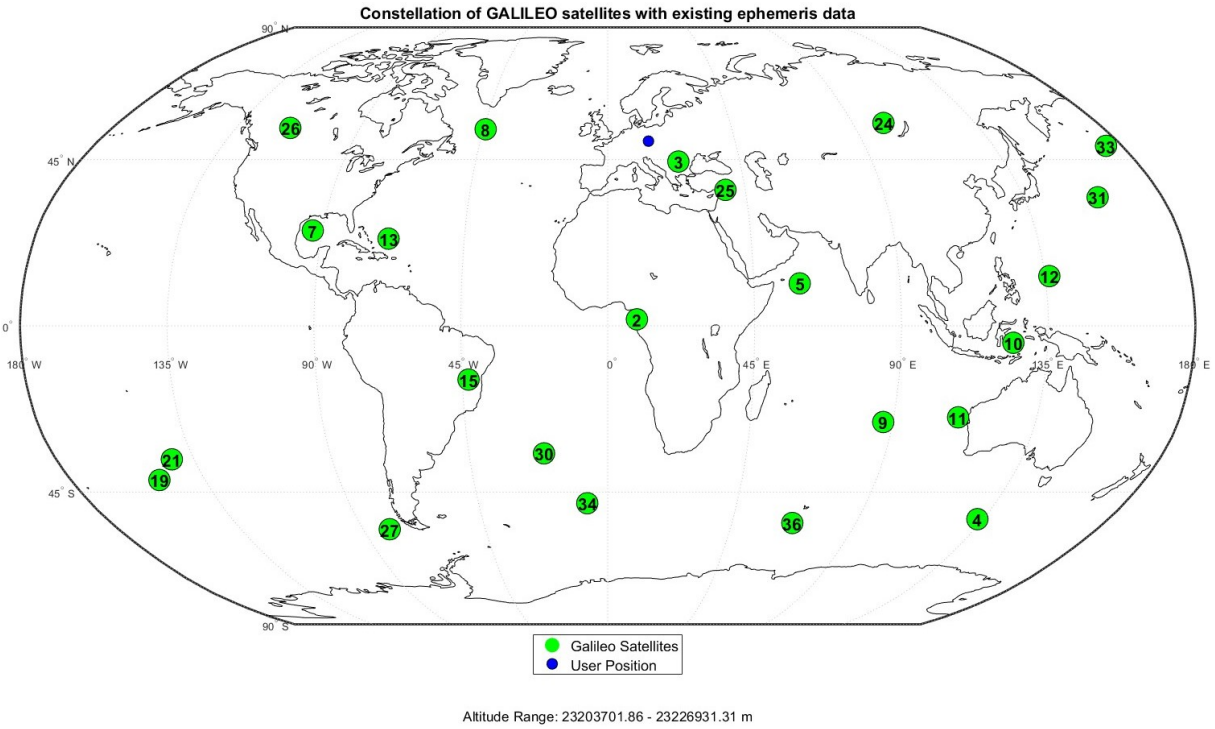

Figure 3.7: Galileo constellation

3.2 Receiver positions

Receiver positions, critical for analyzing the impact of ionospheric delays on positioning accuracy, were uniformly distributed across the globe. A Fibonacci sphere algorithm was employed to generate a set of points ensuring a uniform distribution on a spherical surface. This approach mitigates potential biases arising from clustered receiver locations and provides a more representative assessment of the ionospheric effects on a global scale.

Initially, the Fibonacci sphere algorithm utilizing the golden ratio 3.8 generated coordinates in a spherical coordinate system (radial distance, azimuthal angle, and polar angle). To facilitate further calculations and compatibility with standard geospatial datasets, these spherical coordinates were converted to Cartesian coordinates (X, Y, Z) representing ECEF coordinates. Then, these Cartesian coordinates were transformed into latitudes and longitudes, providing a more intuitive representation of the receiver positions on a map.

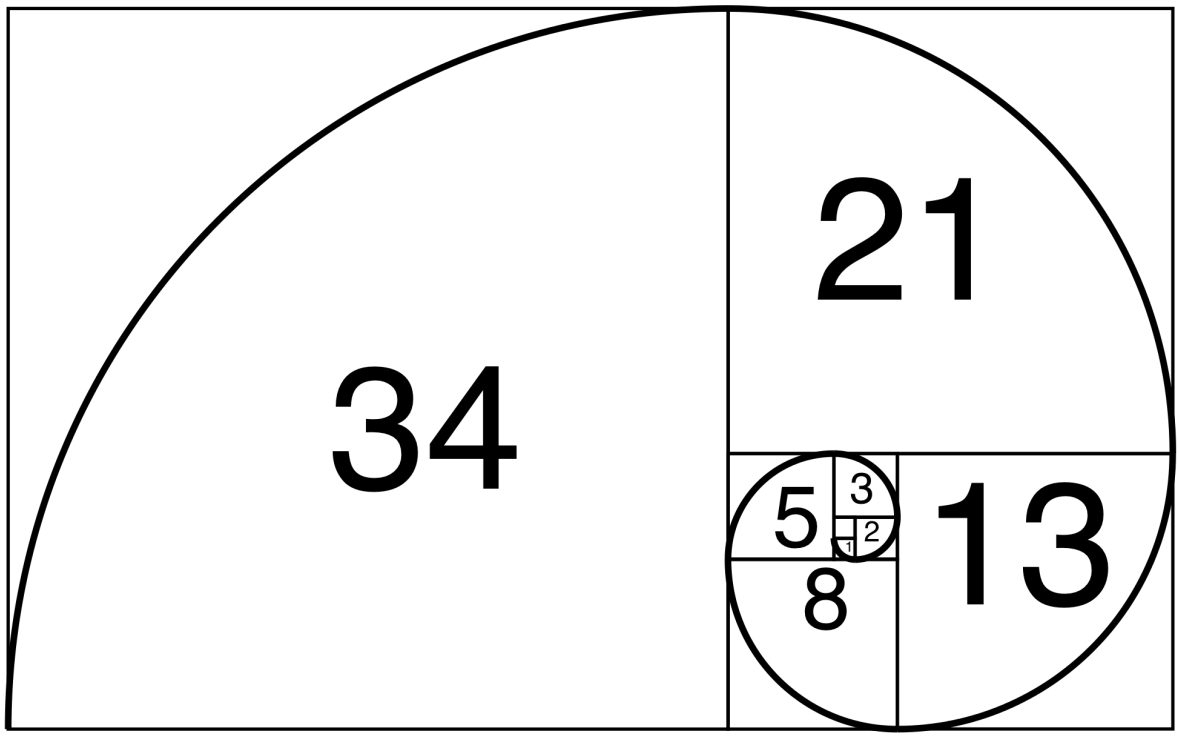

Figure 3.8: Fibonacci spiral

For the initial analysis and demonstration of the methodology, a subset of 20 receiver positions was selected from the uniformly distributed points generated by the Fibonacci sphere algorithm. These 20 positions, shown in figure 3.9, provided a sufficient geographical spread for a initial assessment of the ionospheric impact on positioning. However, to validate the algorithm's performance and ensure its scalability, a more extensive set of 500 receiver positions was also generated using the same Fibonacci sphere approach. This larger dataset, shown in figure 3.10, shows an evaluation of the algorithm's accuracy across a wider range of geographical locations and ionospheric conditions.

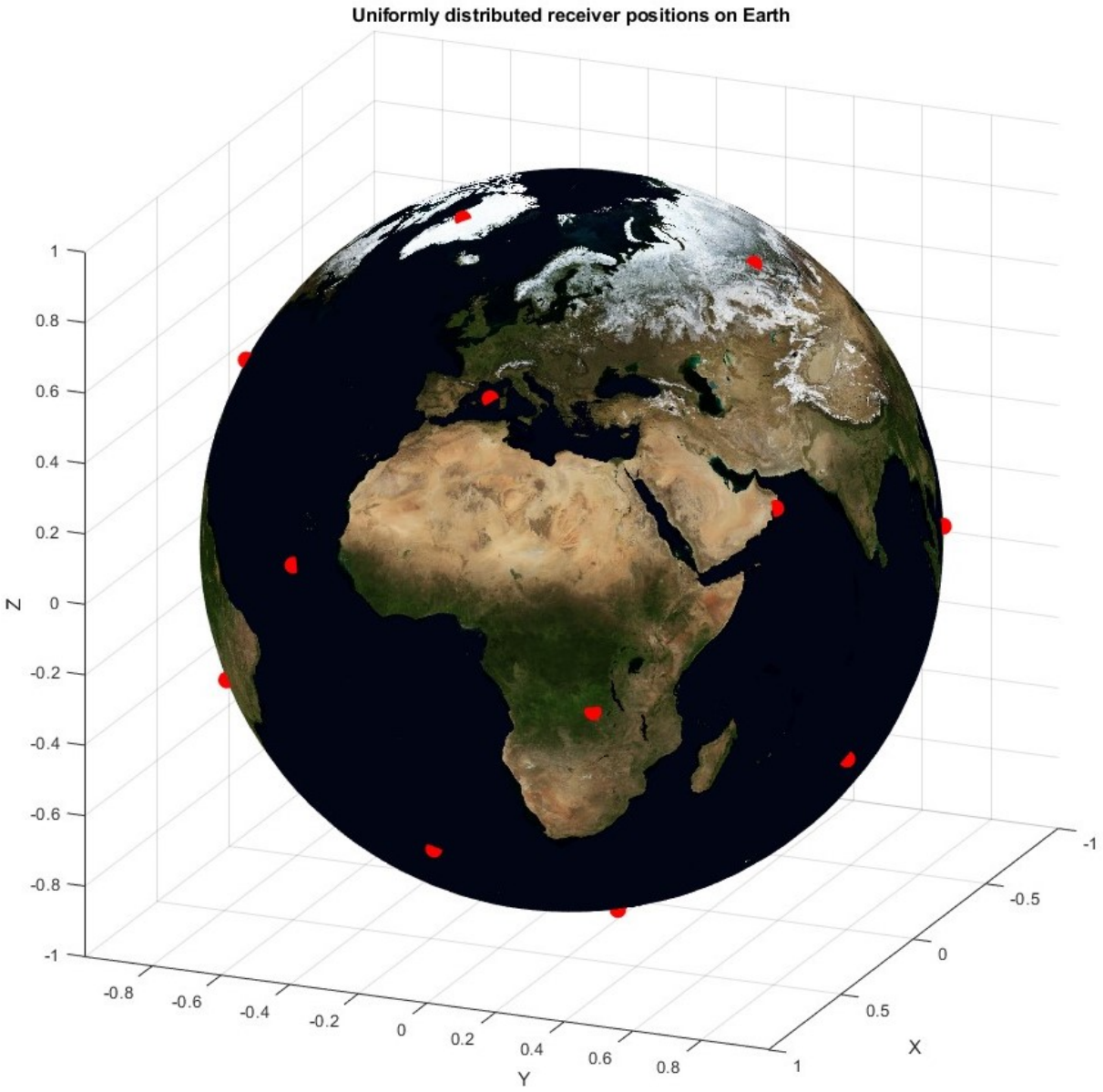

Figure 3.9: 20 uniformly distributed positions

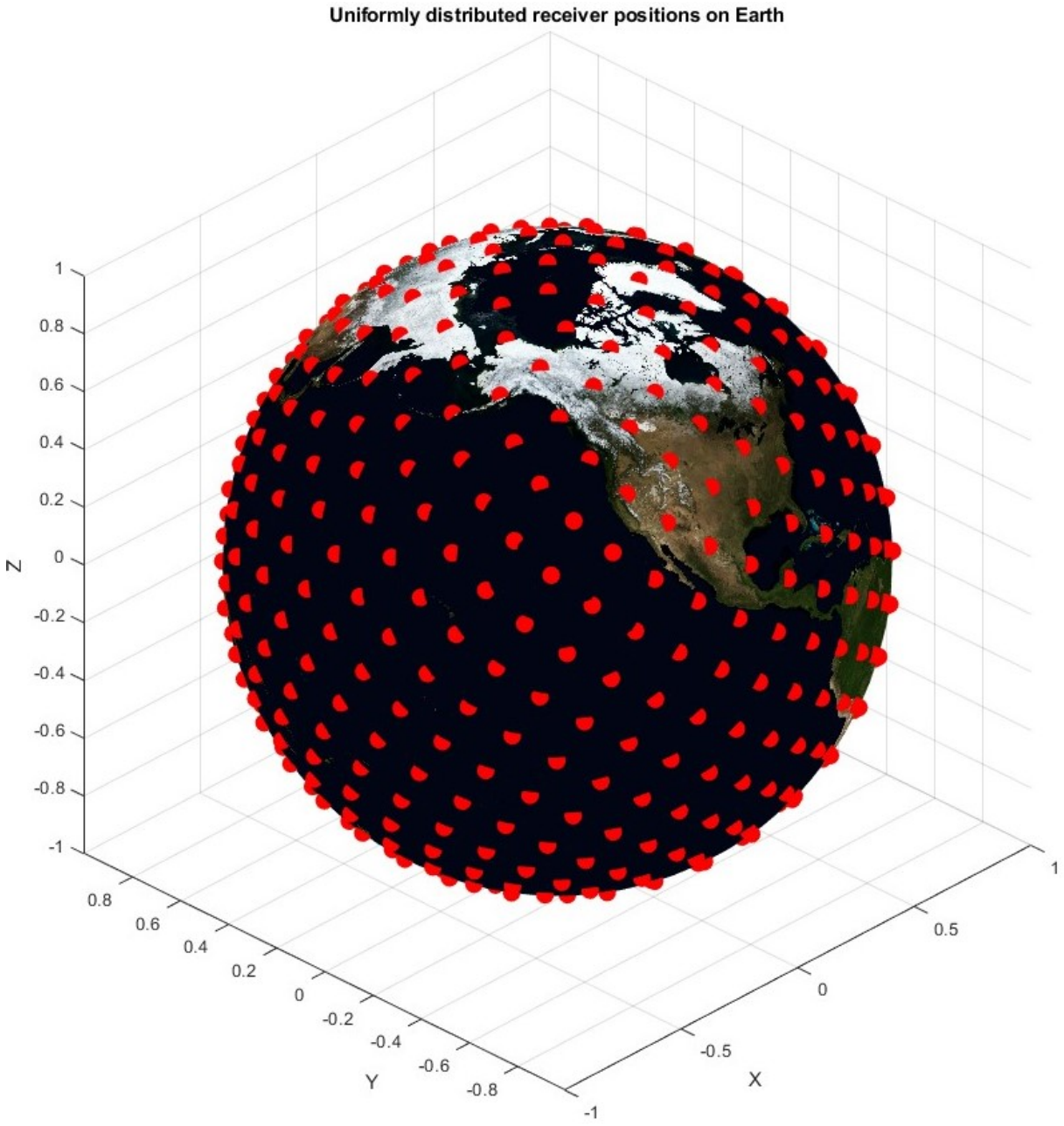

Figure 3.10: 500 uniformly distributed positions

3.3 Visible satellites from each user position

The determination of satellite visibility from each receiver constitutes a crucial step in the process of effectively utilizing GNSS data. This step involves identifying the satellites that are observable from each receiver's position, thus filtering out satellites with potentially obstructed signals. A minimum elevation angle threshold of 5 degrees was employed to ensure that only satellites above this threshold, minimizing the impact of terrestrial

obstacles, were considered visible.

Utilizing the ECEF coordinates of each receiver, azimuth and elevation angles were calculated for each visible satellite. These angles, representing the direction of the satellite relative to the receiver, served as essential inputs for the Klobuchar ionospheric model.

To analyse of the results, the calculated azimuth and elevation angles for each visible satellite were plotted separately for each GNSS constellation. This graphical representation allowed for a clear visualization of the distribution of visible satellites, providing a clear picture of the coverage and accessibility of GNSS signals for different receivers.

3.3.1 Visible GPS satellites

Minimum number of visible GPS satellites were found to be 9, while maximum - 13. It is presented on figure 3.11.

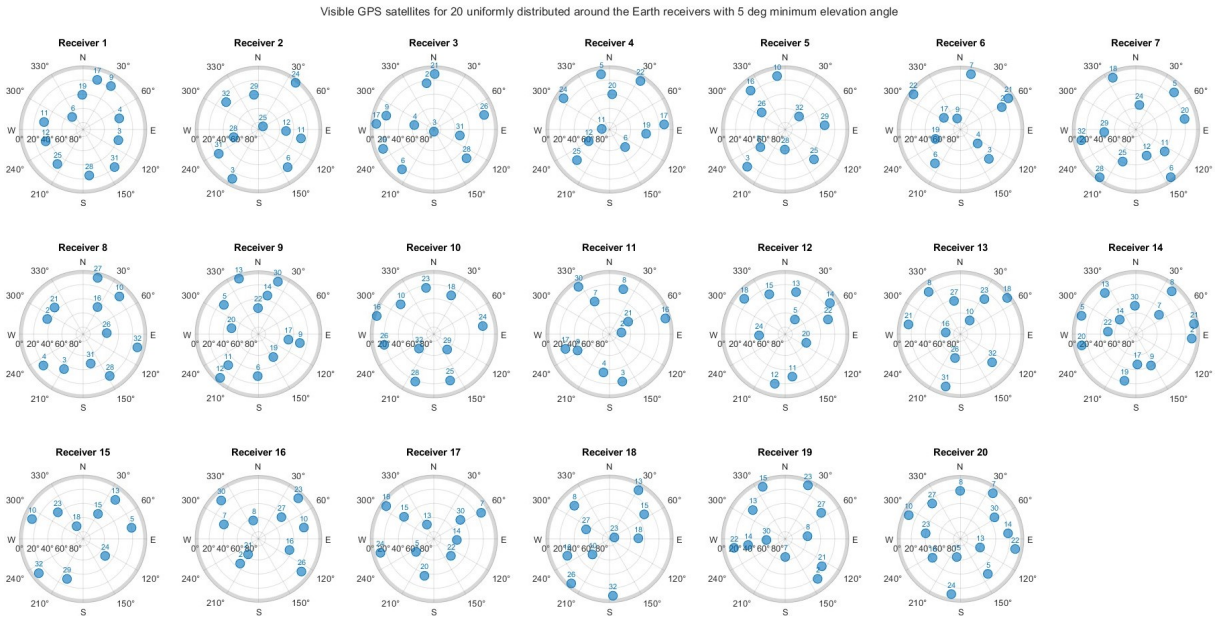

Figure 3.11: Visible GPS satellites for each receiver position

3.3.2 Visible Galileo satellites

Minimum number of visible Galileo satellites were found to be 4, while maximum - 10. It is presented on figure 3.12

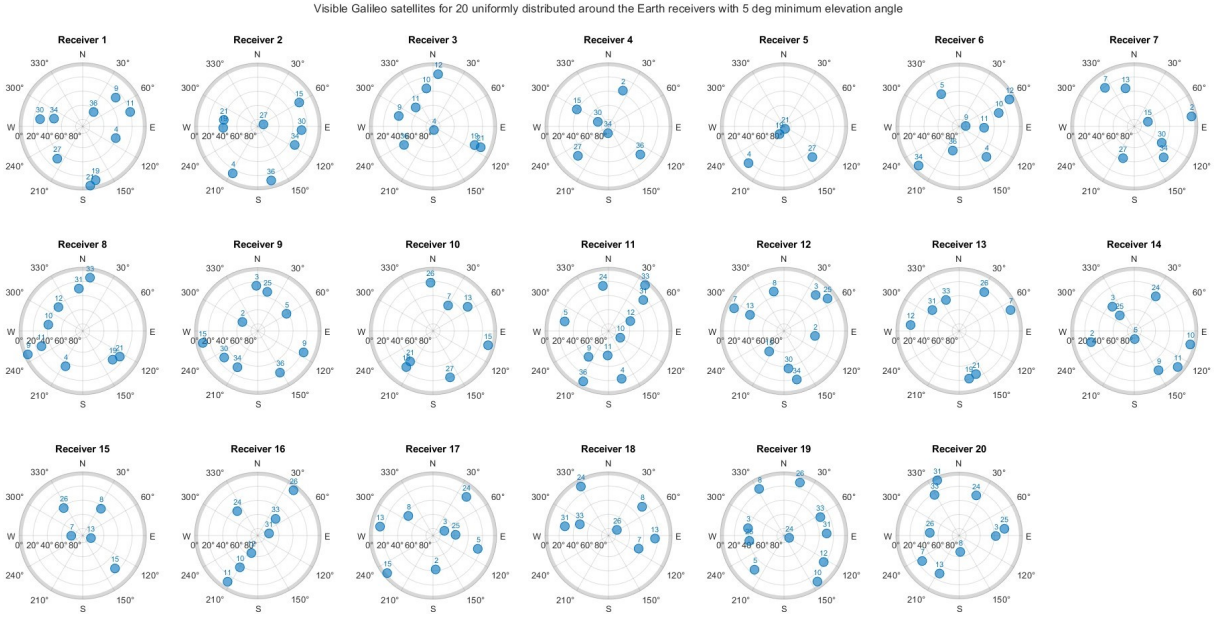

Figure 3.12: Visible Galileo satellites for each receiver position

3.4 Ionospheric models

3.4.1 Klobuchar model

Klobuchar model as inputs uses receiver's geodetic position, viewing a GPS satellite at an azimuth and elevation angles, as well as, UT time and 8 Klobuchar coefficients broadcasted in the RINEX file. After preforming calculation for each receiver and its group of GPS satellites, ionospheric delay was found and example of it for the first receiver is presented in Table 3.1, as well as fully available in the attachments to this work.

Table 3.1: Klobuchar ionospheric delay for receiver position 1 (latitude = -71.805128, longitude = 46.323758)

Satellite	Azimuth (degrees)	Elevation (degrees)	Ionospheric Delay (meters)
1	106.863877	37.984108	2.277338
2	72.884853	36.619522	2.334166
3	318.798430	66.509398	1.598128
4	32.602272	17.154353	3.468996
5	280.786763	33.790969	2.460633
6	252.478944	34.490317	2.428254
7	15.855570	17.143272	3.469833
8	358.554604	40.974043	2.161959
9	216.779072	29.231426	2.690337
10	172.387445	24.526122	2.962998
11	140.073060	20.812779	3.205384

3.4.2 NeQuick model

NeQuick model is issued by request by European GNSS Service Centre.[3]

The model is supplied raw. But for this work it was built in Microsoft Visual Studio 2022. Inputs for the model include time, month, 3 model coefficients broadcasted in the RINEX file and geodetic coordinates of satellites and receivers. STEC was calculated with the use of previously computed Galileo data. Results for the first receiver are presented in Table 3.2. Complete results for each receiver are available in the attachments to the work.

Table 3.2: NeQuick ionospheric delay for receiver position 1 (latitude = -71.805128, longitude = 46.323758)

Satellite	Longitude (degrees)	Latitude (degrees)	STEC (TECU)
1	132.99569	-52.54106	11.56548
2	86.93952	-25.99604	12.11014
3	110.22276	-24.71961	17.04507
4	-150.34507	-41.69388	27.77918
5	-142.27764	-36.08426	34.34988
6	-80.21176	-55.39749	11.83838
7	-20.64303	-34.46119	10.24928
8	-7.11697	-48.08949	8.01555
9	66.97578	-53.63193	7.32659

3.5 NeQuick output conversion

NeQuick model brings results in TECU. Conversion to meters was performed according to equation 2.12, and then compared with Klobuchar and shown in 3.3.

It is important to note that each satellite for each ionospheric model, occupies its own position in space. This difference in satellite positions results in varying slant ranges, the distances between the receiver and the satellite. As a consequence, the ionospheric delay, which is dependent on the slant range, cannot be directly compared between models. This necessitates the implementation of appropriate methods to account for the varying slant ranges when evaluating the impact of ionospheric delays on positioning accuracy. However, this is not discussed in the scope of this work. Data presented below is for review of the models performances.

Table 3.3: Comparison of the ionospheric delays between two models for receiver 1

Satellite	Klobuchar delay (m)	NeQuick delay (m)
1	2.277338	1.877915294251020
2	2.334166	1.966353071512910
3	1.598128	2.767649733913280
4	3.468996	4.510573446476250
5	2.460633	5.577474087343320
6	2.428254	1.922226735177050
7	3.469833	1.664200678835740
8	2.161959	1.301504471654770
9	2.690337	1.189636350216910
10	2.962998	
11	3.205384	

3.6 Comparison of the outputs between the models

Due to the specific scope of this work, a direct comparison of ionospheric delays between the Klobuchar and NeQuick models was not feasible. Instead, a manual observation approach was employed to compare the delays from similarly located satellites above a given receiver. This comparison, while limited in scope, revealed that the NeQuick model generally exhibited higher accuracy compared to the Klobuchar model. This observation aligns with findings from previous research efforts that have similarly demonstrated the superior performance of the NeQuick model. [5]–[7]

Nevertheless, that the data used for this comparison, while not presented in the main body of the text due to its extensive nature, is readily available within the attachments to this work. The data provides information of the observed ionospheric delays for each model and each user, bringing a more detailed analysis and validation of the findings.

3.7 Receivers positions influenced by ionosphere

This section deals with the process of determining receiver positions by incorporating the previously calculated ionospheric delays. This step aims to accurately estimate receiver locations while accounting for the impact of the ionosphere on signal propagation.

As a first step in this process, all available receiver coordinates were converted to ECEF coordinates. This conversion ensured a consistent coordinate system for all receivers for the subsequent calculations. With the receiver coordinates in ECEF, trueranges, which represent the true distances between the receivers and the satellites, were calculated. These trueranges serve as a fundamental input for the positioning algorithms.

To verify the accuracy of the calculated receiver positions, the trueranges were then incorporated into a multilateration algorithm. Two distinct approaches were employed, but the core method remained the same – multilateration.

Concept of the algorithm is shown on figure 3.13.

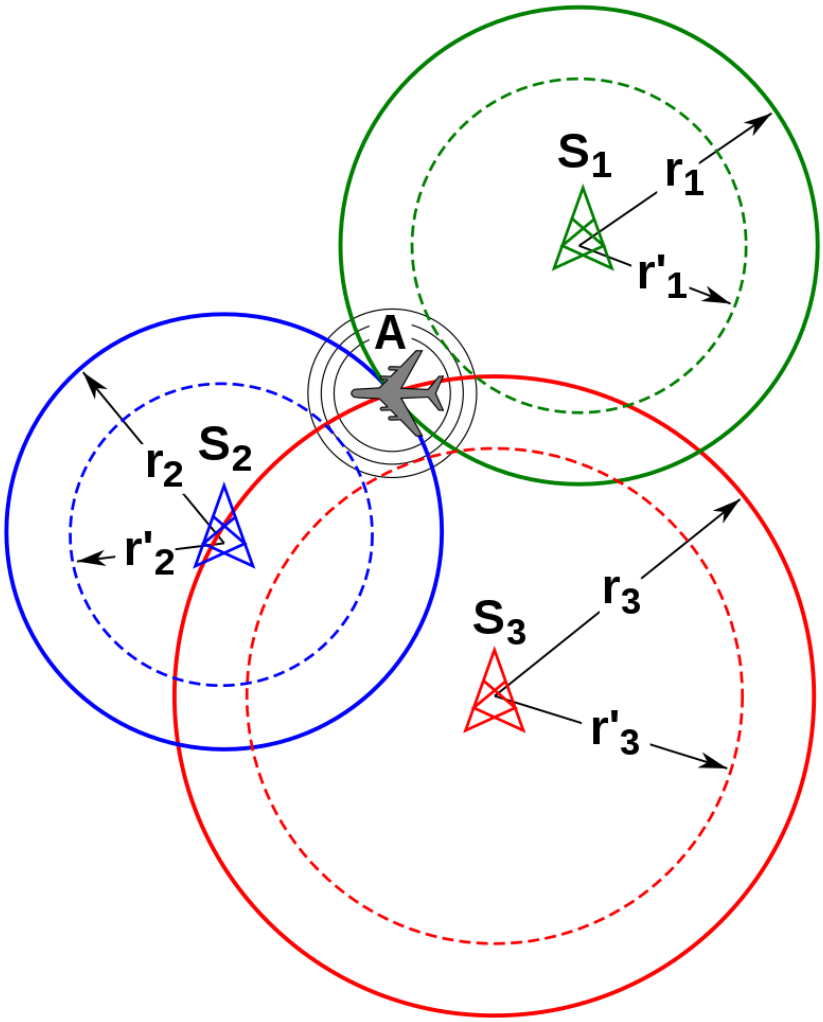

Figure 3.13: Concept of multilateration algorithm

The first approach utilized the actual receiver positions as initial guesses for the algorithm. This approach, as expected, resulted in the same receiver positions as those generated by the Fibonacci sphere algorithm used for receiver distribution.

To gain deeper insights into the correctness of the positioning algorithm, a second approach was employed. In this approach, the initial guesses for the receiver positions were set to the center of the Earth. This allowed the algorithm to derive receiver positions based solely on the trueranges and satellite positions, removing any potential bias introduced by prior knowledge of the receiver locations. The receiver positions derived using this approach, utilizing only trueranges and satellite positions, almost no difference (less than 0.1%) compared to the actual positions. However, to minimize the potential for even the slightest errors, it was decided to proceed with the actual receiver positions for further analysis and comparison.

Then, pseudoranges, which represent the measured distances between the receivers and each satellite, were determined. Pseudoranges typically include various error sources, including tropospheric errors, clock biases, and ionospheric errors. Image representation is shown on 3.14.

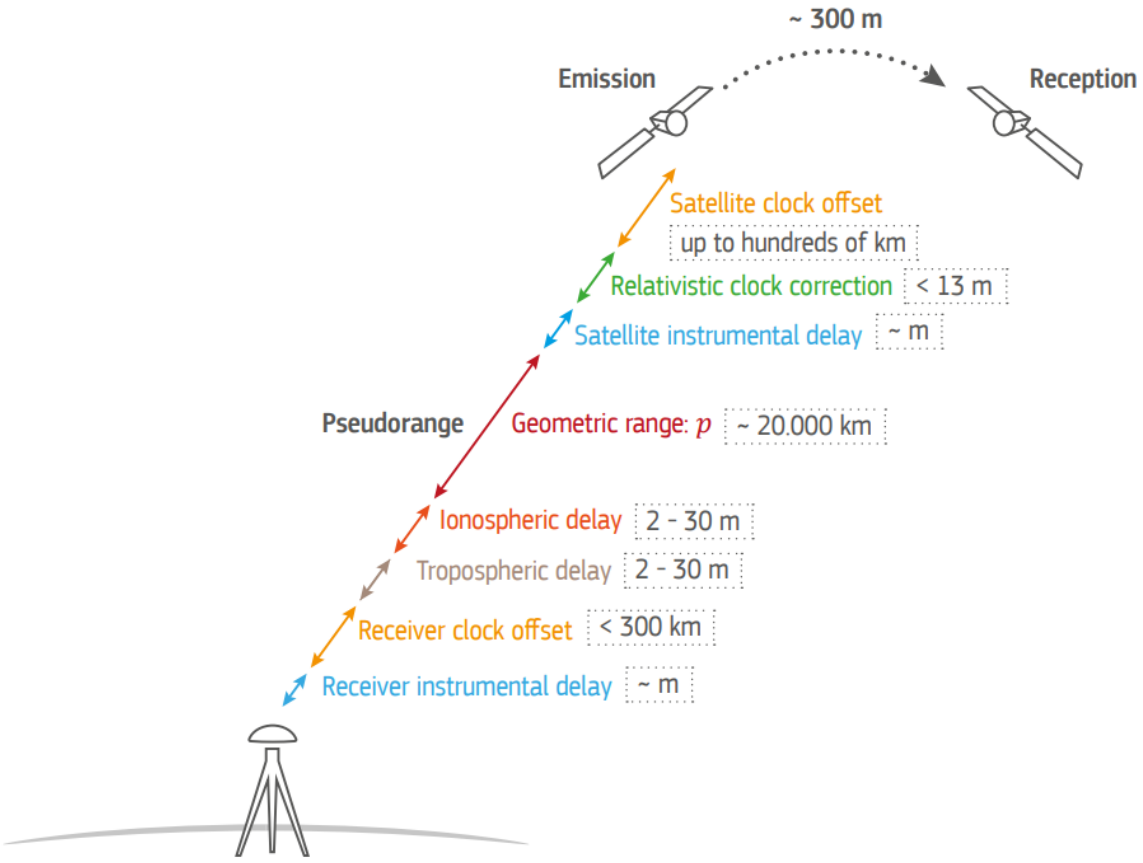

Figure 3.14: Pseudorange

However, due to the specific focus of this work, all errors except for the ionospheric errors were considered negligible and set to zero. Therefore, the pseudorange calculation was simply an addition of the trueranges and the previously calculated ionospheric delays for each satellite-receiver pair. This simplified approach allowed for a focused analysis of the impact of ionospheric delays on positioning accuracy, isolating the effect of the ionosphere on the overall positioning solution.

3.8 Position errors

To quantify the impact of ionospheric delays on receiver positioning accuracy, position errors were investigated. This analysis involved comparing the true receiver positions with the positions obtained after incorporating ionospheric delays. Specifically, the estimated positions with ionospheric delays were subtracted from the true receiver positions, for each receiver and each model independently. The resulting differences in positions, expressed in ECEF coordinates, are presented in table 3.4. This table provides a detailed information of the position errors for each model.

Table 3.4: Position errors (meters) between true receivers positions and influenced by ionosphere on April 17, 2024 at 2:00 UTC across the globe

Receiver	K error X	N error X	K error Y	N error Y	K error Z	N error Z
1	0.66	1.79	0.66	1.27	-3.00	-3.19
2	1.26	0.97	-1.81	-1.70	-7.58	-3.62
3	-0.02	-2.55	3.81	6.30	-9.37	-11.99
4	2.38	0.79	-0.25	0.02	-2.20	-0.68
5	-12.78	-6.67	-10.20	-7.42	-13.20	-11.33
6	2.90	4.95	6.57	6.05	-6.56	-6.41
7	6.76	2.86	-5.85	-9.55	-4.34	-3.14
8	-24.62	-21.40	8.58	7.30	-8.39	-11.07
9	3.27	2.17	1.64	1.50	-0.59	-2.14
10	-5.88	-3.39	-21.03	-13.77	-0.81	-3.45
11	-5.54	-3.99	20.92	15.12	0.26	0.52
12	2.82	16.68	-1.39	-5.95	0.46	2.75
13	-23.77	-28.25	-7.87	-10.30	7.04	6.23
14	7.72	5.55	6.75	4.41	3.51	2.72
15	4.08	0.97	-9.29	-5.46	6.32	5.12
16	-15.27	-11.86	12.08	8.08	14.05	17.09
17	2.57	3.01	0.32	2.30	2.12	7.22
18	-3.40	-2.02	-5.60	-3.39	15.11	6.29
19	2.03	2.26	4.04	3.05	10.09	11.47
20	0.72	1.45	-0.75	-0.50	3.37	4.31

3.9 Transformation between models

As an initial step into the transformation between the Klobuchar and NeQuick ionospheric models it was decided to perform direct transformation of the broadcasted coefficients.

Utilization of the all available data from 280th day of year 2015 to 107th day of year 2024 was done. All the broadcasted messages are not included in the attachments to the work due to their size, but they are openly available on Internet. Only Klobuchar and

NeQuick coefficients are included in the work since method is based only on the coefficients transformation.

Coefficients were extracted from every available RINEX file and are attached to the work. All days with missing data were also excluded in the scope of transformation to mitigate the potential errors. Two approaches were made: linear regression with ridge regularization and incorporating a feedforward neural network.

3.9.1 Linear regression with ridge regularization

This method splits the data into training and testing sets, performs correlation analysis, and selects features based on correlation coefficients. It relies on traditional linear regression techniques with feature selection based on correlation analysis. Linear regression model was fitted using the least squares approach. The least squares approach can be used to fit models that are not linear models. Model was set to 80% training and 20% testing. Correlation matrix was developed and showed small correlation between the coefficients and can be accessed in 3.5.

Table 3.5: Correlation Matrix

1	-0.19	0.05
-0.19	1	0.1
-0.05	0.1	1

Weak correlations suggests that the variables are not strongly related to each other in a linear manner.

After several attempts, successful transformation was not found. Difference between actual and predicted coefficients from -10% to -172%. Only second and sixth Klobuchar coefficients were predicted with relatively acceptable difference from real coefficients of -10%.

3.9.2 Neural network

This method was utilizing a feedforward neural network. Advantages of this method is that it potentially can capture nonlinear relationships between inputs and outputs, offering more flexibility in modeling complex patterns in the data. The entire dataset was normalized using min-max normalization. The model was trained on all available data. The architecture of the neural network was specified with two hidden layers, each containing 10 neurons. However, more neurons, up to 100 in each layer, were also incorporated

for potentially better results, but did not bring significant changes and only made computation more complex. Attempts on increasing hidden layers were also performed, but did not show improvement.

Network diagram can be seen on figure 3.15.

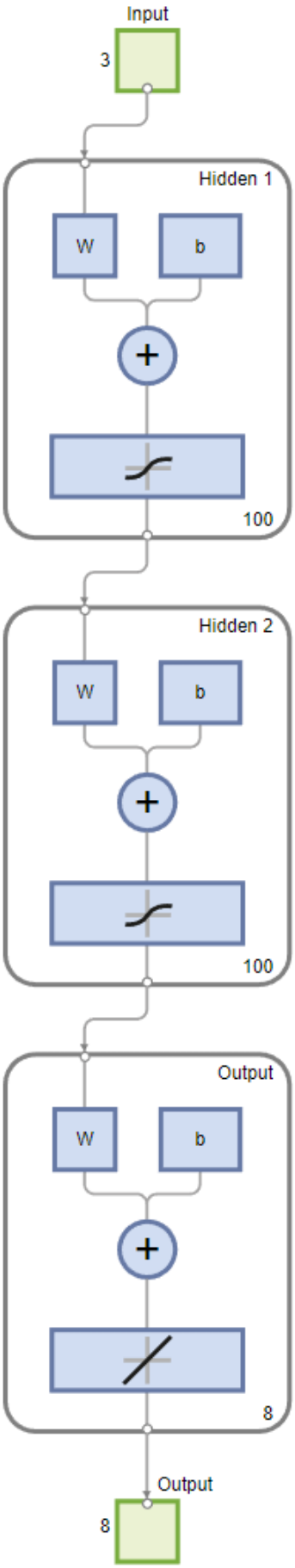

Figure 3.15: Neural network diagram

Computational complexity of the potentially acceptable results can be seen on figure 3.16. For one attempt of transformation with relatively low complexity, neural network training may take up to 30 minutes on a up to 4 GHz 8 logical cores CPU. Although, a well trained model can be saved and utilized later.

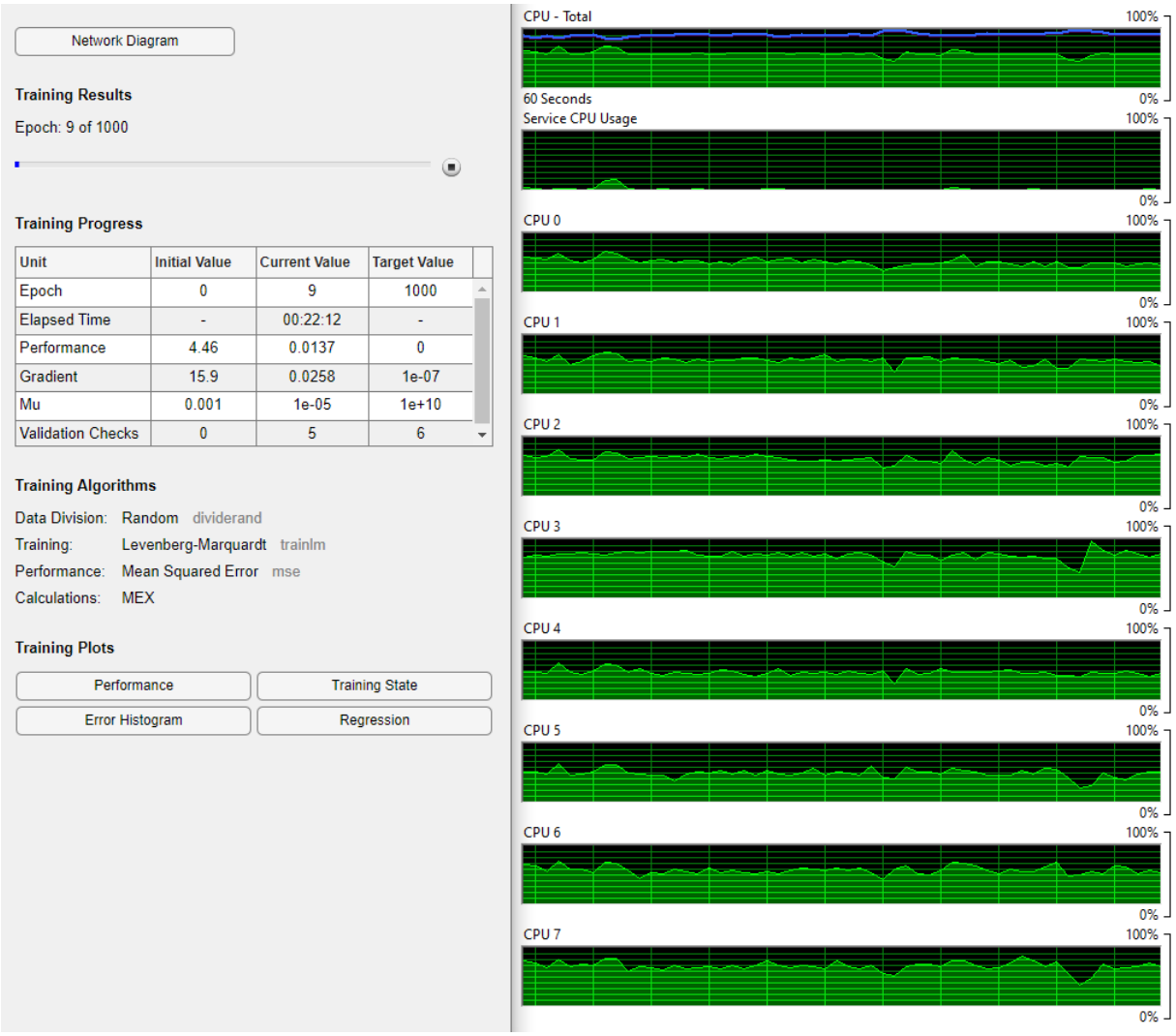

Figure 3.16: Neural network interface

Training algorithms such as Levenberg-Marquardt (LM), Bayesian Regularization (BR), Resilient Backpropagation (RB), Scaled Conjugate Gradient (SCG), Conjugate Gradient with Powell/Beale Restarts (CGwPBR), Fletcher-Powell Conjugate Gradient (FPCG), Polak-Ribiere Conjugate Gradient (PRCG), One Step Secant (OSS), Variable Learning Rate Gradient Descent (VLRGD), Gradient Descent with Momentum (GDwM), Gradient Descent (GD) were utilized. Performance of each training algorithm was assessed and results of assessment showed that Bayesian Regularization and Levenberg-Marquardt training algorithms performed the best for model transformation. Performance data can

be seen on table 3.6

Table 3.6: Comparison of optimization algorithms

Original	3.63E-08	7.45E-09	-1.79E-07	-5.96E-08	1.39E+05	3.28E+04	-3.28E+05	3.28E+05
GD	2.65E-08	1.68E-08	-1.30E-07	-1.23E-07	1.22E+05	-1.02E+05	-7.55E+04	-5.51E+04
GDwM	-6.25E-10	6.31E-08	5.63E-08	1.19E-07	2.98E+05	-1.12E+05	-9.54E+05	9.25E+05
VLRGD	2.22E-08	1.12E-08	-1.18E-07	-2.30E-09	1.28E+05	3.19E+04	-1.63E+05	4.20E+04
OSS	2.43E-08	1.22E-08	-1.28E-07	-2.22E-08	1.31E+05	2.52E+04	-1.87E+05	5.33E+04
PRCG	2.41E-08	1.42E-08	-1.23E-07	-4.78E-08	1.30E+05	5.31E+04	-2.05E+05	1.14E+04
FPCG	2.35E-08	1.49E-08	-1.25E-07	-3.90E-08	1.28E+05	5.48E+04	-1.87E+05	-3.14E+04
CGwPBR	2.07E-08	1.14E-08	-1.20E-07	-2.50E-08	1.24E+05	5.51E+04	-1.86E+05	8.52E+04
SCG	2.12E-08	1.27E-08	-1.18E-07	-3.16E-08	1.23E+05	4.14E+04	-1.96E+05	6.28E+04
RB	2.55E-08	1.49E-08	-1.26E-07	-4.07E-08	1.30E+05	3.86E+04	-1.88E+05	-2.58E+04
BR	2.44E-08	1.30E-08	-1.31E-07	-3.24E-08	1.30E+05	3.46E+04	-2.22E+05	5.61E+04
LM	2.43E-08	1.43E-08	-1.20E-07	-3.37E-08	1.32E+05	2.14E+04	-2.31E+05	1.02E+05

Performance of the network with Levenberg-Marquardt algorithm is shown on figure 3.17.

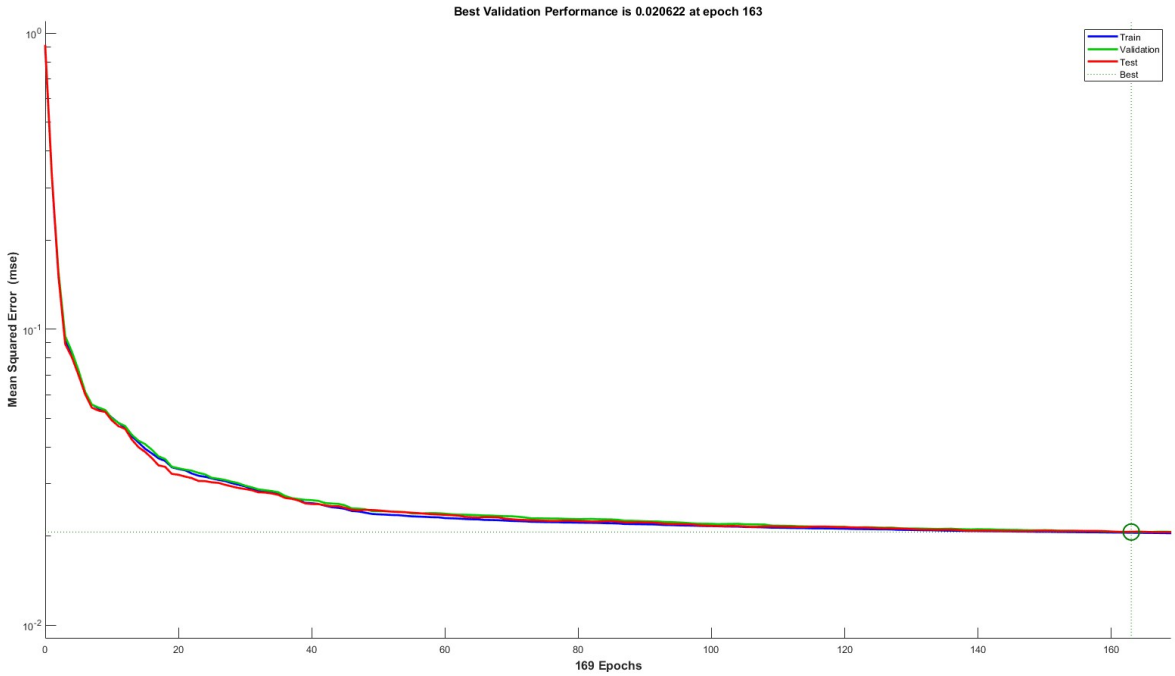

Figure 3.17: Performance of the model

Training state can be investigated on figure 3.18.

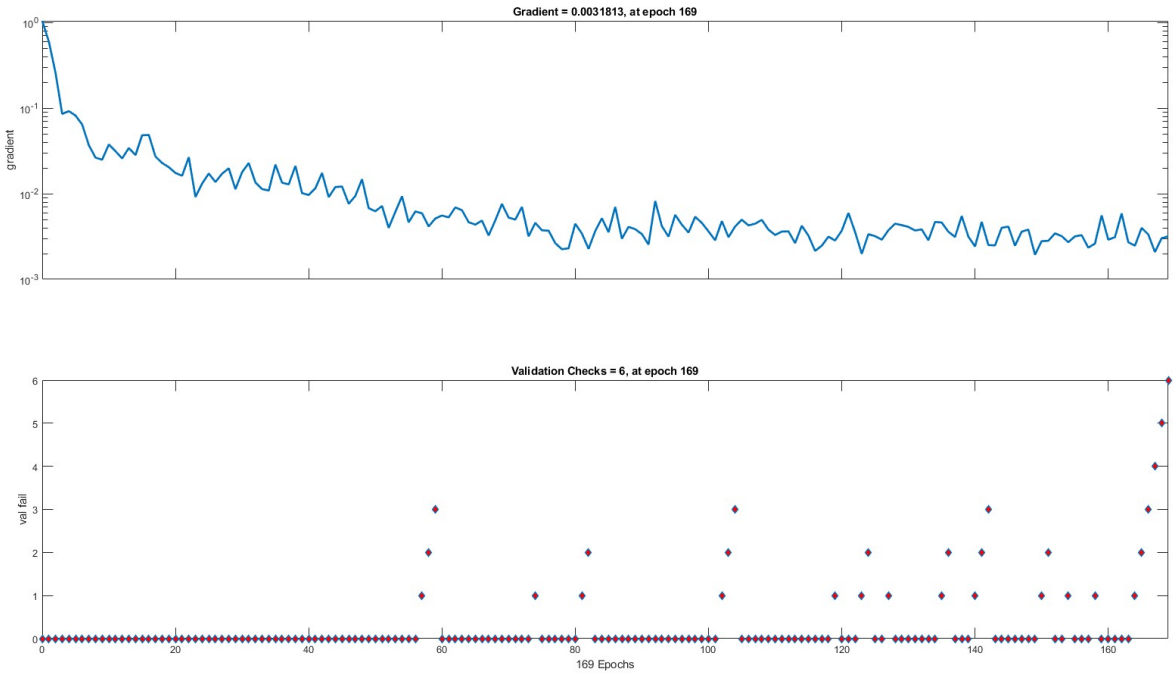

Figure 3.18: Training state of the model

Error histogram is presented on figure 3.19.

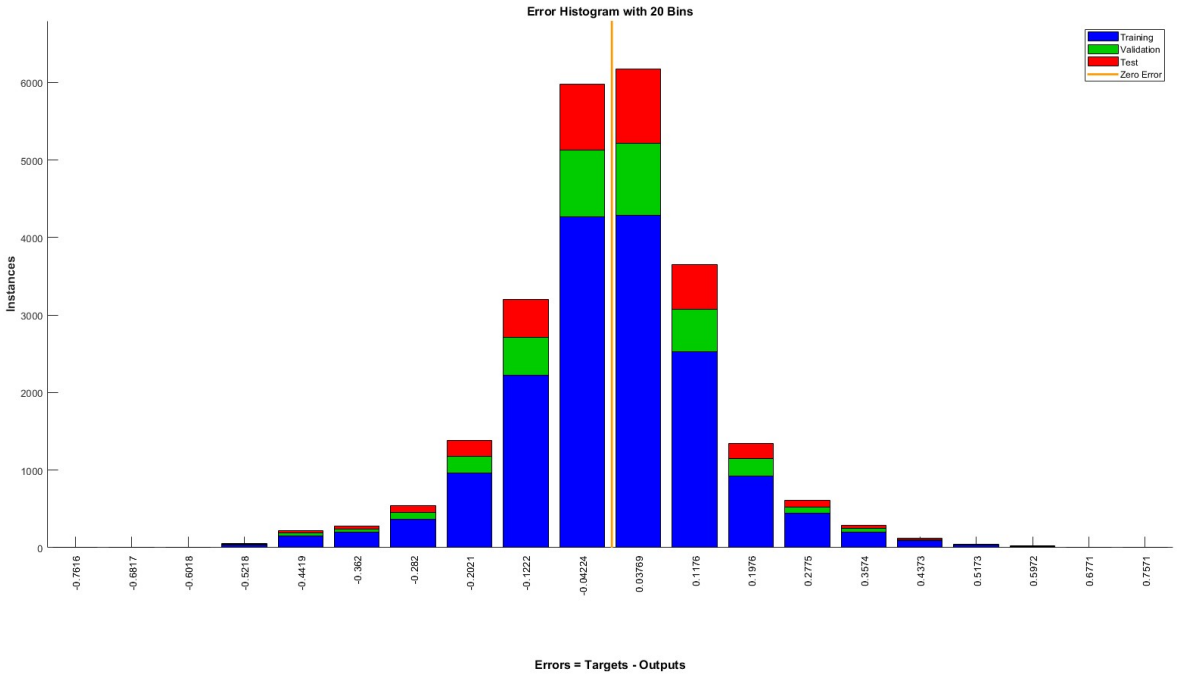

Figure 3.19: Error historgram of the model

Regression is shown on figure 3.20.

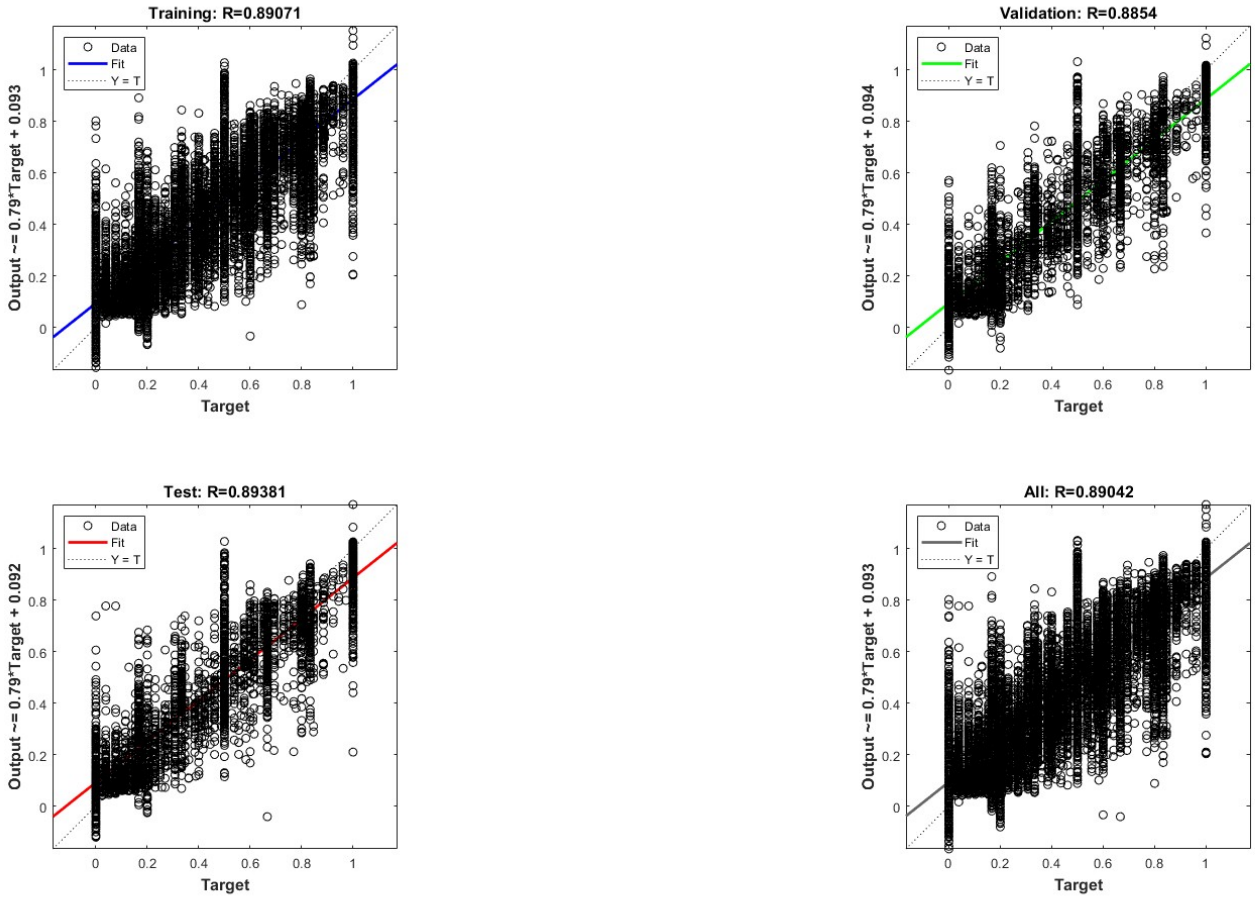

Figure 3.20: Regression

The attempts on better neural network training were also made, however, even after long time (up to 1 hour) of training, the difference between initial model was not seen, so rest of the attempts were performed with smaller data training time due to extensive use of computational resources.

Using the Bayesian Regularization on random days and coefficients showed potentially good performance for some of the coefficients. Sometimes even predicting the coefficients exactly as they are supposed to be or in an acceptable margin. However, the performance was not steady. Difference between actual and predicted coefficients for random 10 days are presented in 3.7

Table 3.7: Difference between actual and predicted coefficients

Year	Day	Difference between actual and predicted coefficients							
2024	108	32.78%	74.50%	26.82%	45.64%	6.47%	5.49%	32.32%	82.90%
	107	33.25%	30.19%	22.82%	52.17%	5.49%	198.37%	18.86%	118.32%
	1	11.05%	18.41%	34.98%	28.14%	2.64%	15.30%	20.91%	145.49%
	45	61.31%	15.19%	29.77%	336.74%	28.77%	387.14%	INF	141.45%
	95	1.35%	19.68%	0.09%	44.06%	3.40%	78.41%	14.19%	72.96%
2020	265	17.32%	10.23%	0.48%	79.17%	0.79%	260.15%	21.45%	427.14%
	238	22.72%	12.95%	0.24%	9.92%	8.14%	112.89%	42.99%	51.30%
	313	32.28%	67.57%	36.56%	12.51%	16.51%	3.95%	36.35%	24.56%
2015	281	39.52%	257.05%	39.96%	281.56%	24.33%	0.00%	8.71%	1021.84%
	365	19.00%	21.50%	15.86%	1.76%	2.59%	33.73%	39.42%	50.73%

As the other potential improvement of the algorithm, removing of all the days with one of coefficient equal to zero was done. This approach did not bring any significant changes to the prediction model.

No further attempts were introduced mostly due to time related resources related. Nevertheless, this initial step into transformation between the models showed that on a random selection of days, 5 of the Klobuchar coefficients may be predicted from the 3 NeQuick coefficients to high extent. Other 2 coefficients lay in a margin of 10% and only last 8th predicted Klobuchar coefficient shows large difference with the actual data from GPS navigation message.

Chapter 4

Conclusion

The transformation between the Klobuchar and NeQuick ionospheric models shows a complex challenge due to the fundamental differences and different relationships between models coefficients. This study explored two approaches: linear regression with ridge regularization fitted using the least squares approach and a feedforward neural network with different numerous training algorithms.

While linear regression showed a weak correlations between the coefficients and low prediction accuracy, the neural network approach demonstrated a potential for capturing relationships between the coefficients. Although, regardless extensive training and optimization, the network struggled to consistently predict all of the coefficients to a satisfactory degree.

The study provides good results for five of the Klobuchar coefficients, which could be predicted from the real NeQuick coefficients with high accuracy on certain days. However, further refinement and enhancements is necessary to achieve consistent and reliable prediction across all of the coefficients and a wider range of conditions.

The results suggest that an improvement of neural network techniques could potentially improve transformation accuracy. Future research may explore this direction along with investigating additional data pre-processing and model parameterization techniques to optimize performance.

Despite the challenges, this work laying the groundwork for further research into the transformation between the Klobuchar and NeQuick models. With continued exploration and optimization it might be possible to develop an accurate and robust algorithm for transformation between the two ionospheric models.

The development of an accurate and reliable transformation algorithm might have positive influence for real-time ionospheric modeling and navigation applications. It may enable the seamless integration of data from different ionospheric models, providing more accurate and reliable navigation information for users worldwide, as ionosphere remains the single largest contributor to GNSS positioning errors, especially for single-frequency receivers.

Appendix A

Attachments

Attachments contain an archive ”attachments.zip”.

Bibliography

[1] B. Hofmann-Wellenhof, H. Lichtenegger, and J. Collins, *Global Positioning System: Theory and Practice*, Book, 2001.

[2] U. D. of Transportation, *IS-GPS-200N Interface Specification for NAVSTAR Global Positioning System (GPS) Space Segment-Navigation User Interfaces*, Technical Report, 2006. [Online]. Available: `https://www.gps.gov/technical/icwg/IS-GPS-200N.pdf`.

[3] E. S. Agency, *Galileo Ionospheric Model*, Technical Report, 2019. [Online]. Available: `https://www.gsc-europa.eusitesdefaultfilessitesallfilesGalileo_Ionospheric_Model.pdf`.

[4] J. A. Klobuchar, "Ionospheric Time-Delay Algorithm for Single-Frequency GPS Users", *IEEE Transactions on Aerospace and Electronic Systems*, vol. AES-23, no. 3, pp. 325–331, 1987. DOI: `10.1109TAES.1987.310829`.

[5] P. d. T. Setti Junior, D. B. M. Alves, and C. M. d. Silva, "Klobuchar and Nequick G Ionospheric Models Comparison for Multi-GNSS Single-Frequency Code Point Positioning in the Brazilian Region", *Boletim De Ciencias Geodesicas*, vol. 25, no. 3, e2019016, 2019. DOI: `10.1590s1982-21702019000300016`. [Online]. Available: `https://doi.org10.1590s1982-21702019000300016`.

[6] A. Farah, "Comparison of GPS/Galileo single frequency ionospheric models with vertical TEC maps", *Artificial satellites*, vol. 43, no. 2, pp. 75–90, 2008.

[7] X. Ren *et al.*, "Global ionospheric modelling using multi-GNSS BeiDou, Galileo, GLONASS and GPS", *Scientific reports*, vol. 6, no. 1, p. 33 499, 2016.

[8] K. Su, S. Jin, and M. M. Hoque, "Evaluation of ionospheric delay effects on multi-GNSS positioning performance", *Remote Sensing*, vol. 11, no. 2, p. 171, 2019.

[9] M. Hernandez-Pajares, J. M. Juan, J. Sanz, *et al.*, "The IGS VTEC maps: a reliable source of ionospheric information since 1998", *Journal of Geodesy*, vol. 83, pp. 1–10, 2009. DOI: `10.1007s00190-008-0266-1`. [Online]. Available: `https://doi.org10.1007s00190-008-0266-1`.

[10] R. Ezquer, L. Scida, Y. Orue, *et al.*, "NeQuick 2 total electron content predictions for middle latitudes of North American region during a deep solar minimum", *Journal of Atmospheric and Solar-Terrestrial Physics*, 2017.